Математический центр в Академгородке

Руководители семинара

Актуальные проблемы прикладной математики

Интернет-семинар 08-05-2020

И.А. Тайманов, С.И. Кабанихин, А.Е. Миронов, М.А. Шишленин.

Математическая иммунология: актуальные задачи моделирования

Г.А. Бочаров

Институт вычислительной математики им. Г.И. Марчука РАН

Отделение Московского центра фундаментальной и прикладной математики в ИВМ РАН

Институт персонализированной медицины Первого Московского государственного медицинского университета имени И.М. Сеченова

SECHENOV UNIVERSITY

Outline

Исследование робастности защиты системой интерферона при коронавирусной инфекции мышей

Идентификация новых мишеней для противовирусной терапии ВИЧ-1

Предсказание терапевтического эффекта блокады рецептора PD-1 в хроническую фазу ВИЧ-1 инфекции

Исследование влияния подвижности Т-лимфоцитов в лимфатическом узле на эффективность элиминации зараженных клеток при ВИЧ-1 инфекции

Геометрическое моделирование структурно-функциональной организации лимфатических узлов

The Immune System

1)

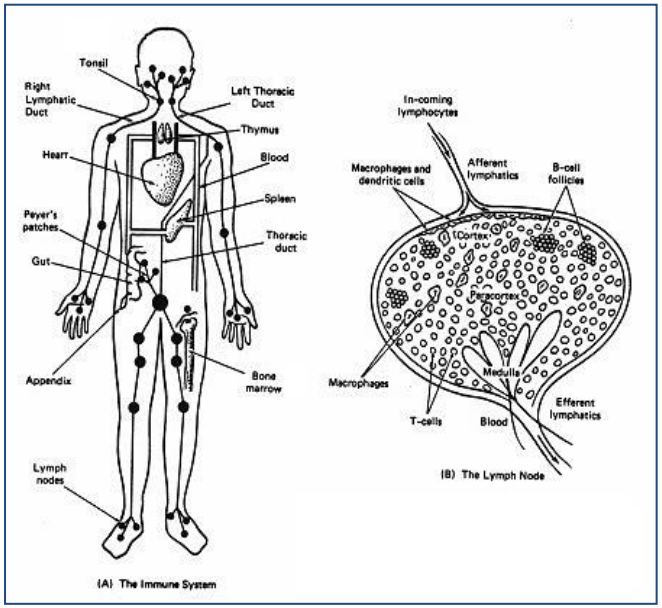

Physical

•Transport

(1% of cells traverse the whole lymphoid system per hour)

•Diffusion

Chemical

• Ligand-receptor

• Signal transduction

• Peptide synthesis

Biological

•Gene regulation

•Generation of antigen receptor diversity

•Cell division (~6 hrs)

•Cell differentiation

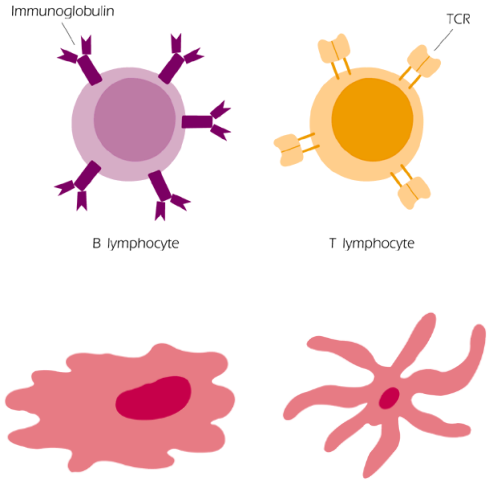

2)

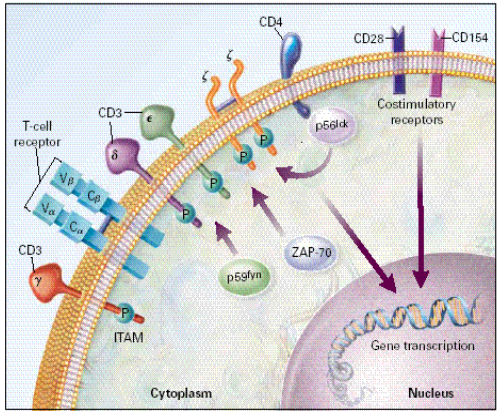

3)

- **Sources of heterogeneity**:

1) *Physical compartments (lymph node, spleen, blood, etc.)*
2) *Distinct cell populations (e.g. lymphocytes, Macrophages)*
3) *Heterogeneity w.r.t. the expression of specific markers (CCR5) or fluorescent labels (CFSE, BrdU)*
4) *…*

The fundamental challenge to applied mathematicians is to understand immunology in new ways by using models, computational techniques & algorithms

Multiscale techniques in immunology: modelling in demand

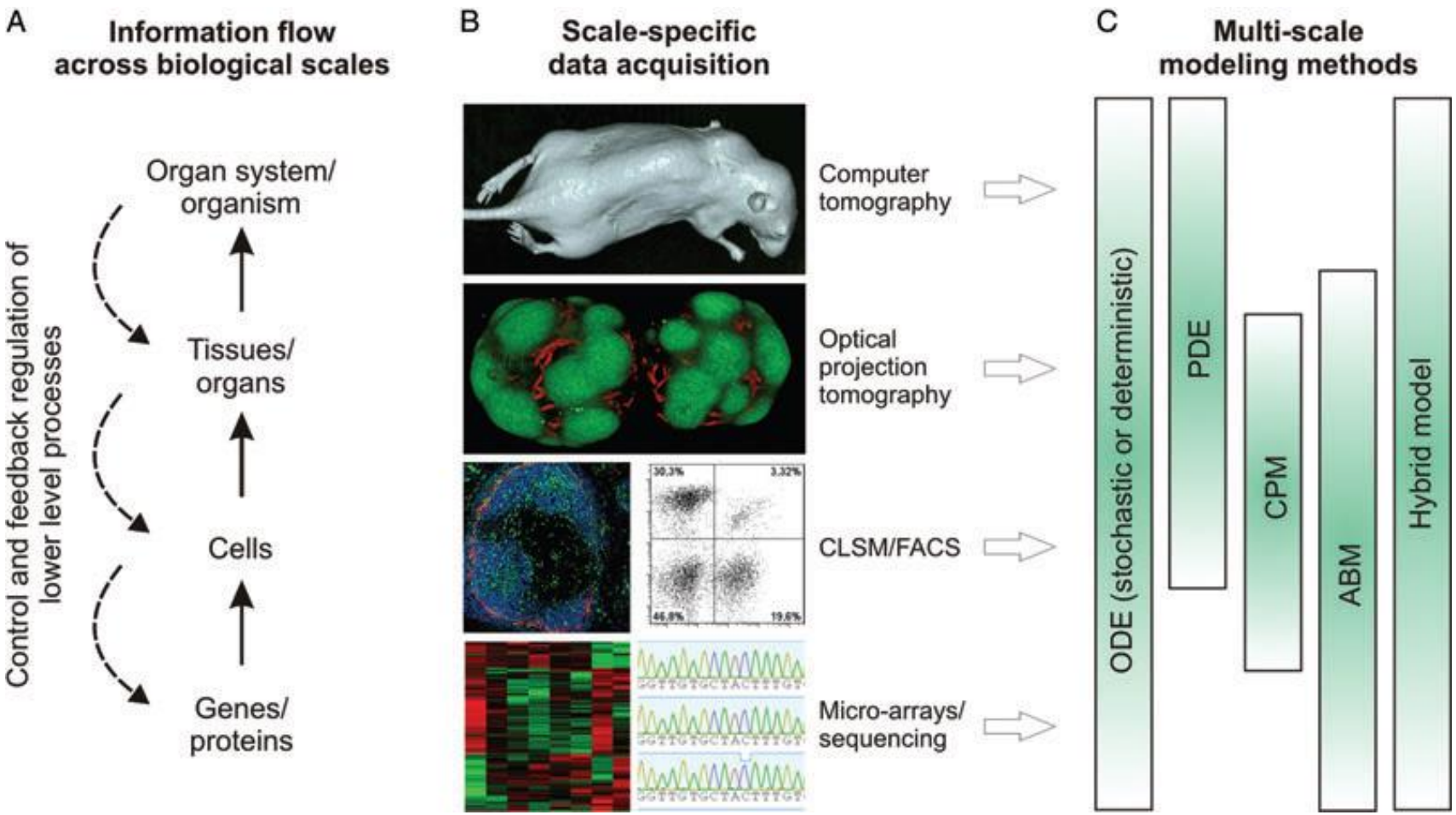

From: *Ludewig et al. Eur J Immunol. 2012 , 42:3116*

Modelling in immunology: Linking Experimental and Mathematical Approaches

Nobel Prize Laureate
Rolf M. Zinkernagel

Academician
Guri I. Marchuk

"…The many immunological observations and results from in vitro or in vivo experiments vary and their interpretations differ enormously. A major problem is that within a normal distribution of biological phenomena that are measurable with many methods virtually anything can be shown or is possible.." *R. M. Zinkernagel. Immunity Against Infections & Vaccines: Credo 2004. Scand J Immunol. 2004, 60: 9–13*

„The outcome of infection results from the ´*numbers games*´ between infectious agent and the immune system."

„Numbers game“: virus & host factors in the outcome of infection

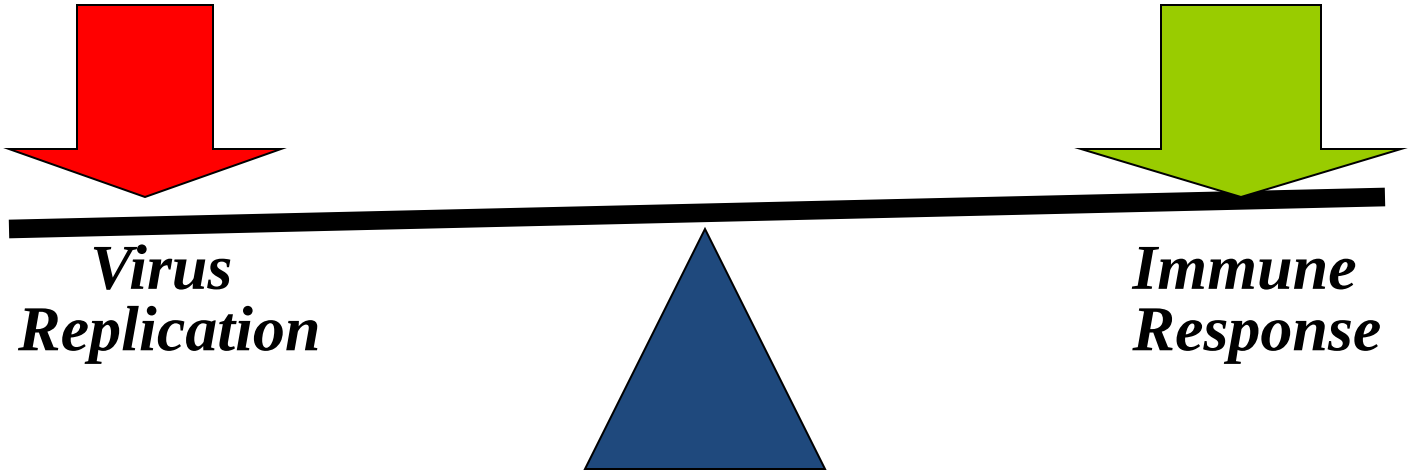

The clinician‘s perspective:

- Cytopathicity of virus
- Latency
- Persistence
- Replication rate
- Tropism
- Immunopathology
- Health condition of the infected individual

The mathematical view:

$$\frac{d}{dt}V(t) = (\beta - \gamma \cdot F(t)) \cdot V(t)$$

$$\frac{d}{dt}F(t) = \rho \cdot C(t) - \eta \cdot \gamma \cdot F(t) \cdot V(t) - \mu_f \cdot F(t)$$

$$\frac{d}{dt}C(t) = \xi(m) \cdot \alpha \cdot V(t-\tau) \cdot F(t-\tau) - \mu_f \cdot (C - C^*)$$

$$\frac{d}{dt}m(t) = \sigma \cdot V(t) - \mu_m \cdot m(t)$$

$$V(t_0) = V_0, \quad F(t_0) = F_0, \quad C(t_0) = C_0, \quad m(t_0) = m_0,$$
$$V(t) = 0, \quad F(t) = F_0 \quad \text{при} \quad t \in [t_0 - \tau, t_0)$$

Physiologically-relevant "questions":
pathogenesis of infectious diseases

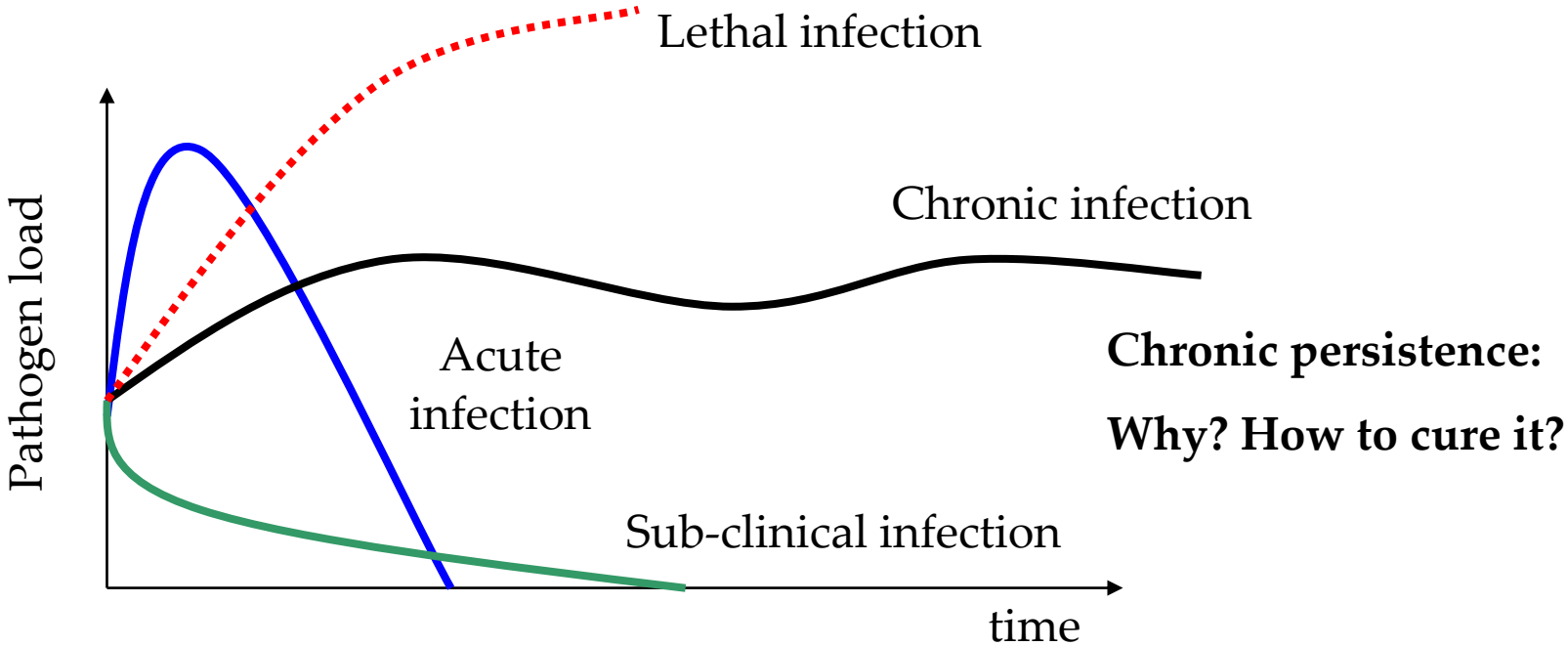

Insights by G.I. Marchuk, I.B. Pogozhev, L.N. Belykh, A.L. Asachenkov, S.M. Zuev, A.A. Romanukha, N.V. Pertcev

- Definition of immunological barrier against infection
- Sufficient stability conditions for chronic steady states
- Treatment of chronic infections via exacerbation

Outline

Исследование робастности защиты системой интерферона при коронавирусной инфекции мышей.

Идентификация новых мишеней для противовирусной терапии ВИЧ-1.

Предсказание терапевтического эффекта блокады рецептора PD-1 в хроническую фазу ВИЧ-1 инфекции.

Исследование влияния подвижности Т-лимфоцитов в лимфатическом узле на эффективность элиминации зараженных клеток при ВИЧ-1 инфекции.

Геометрическое моделирование структурно-функциональной организации лимфатических узлов.

Question to address

- **Innate immune response: <u>limits of protection</u>**
- **<u>How robust is the type I IFN mediated protection against severe cytopathic virus infection?</u>**

Influenza A virus infection: deadly 1918 virus vs Tx/91 mutant

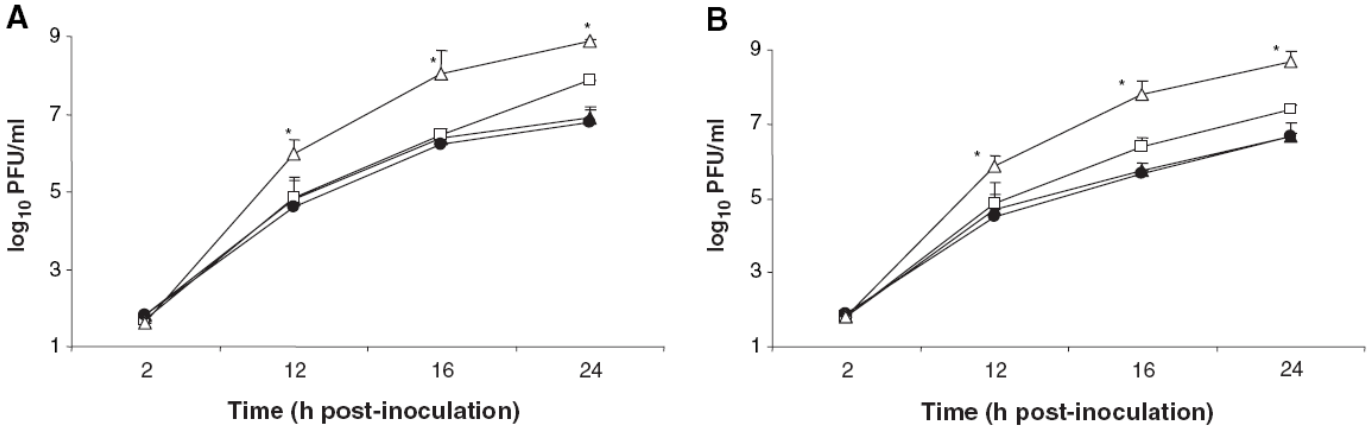

Fig. 3. Release of 1918 influenza virus from apically infected human bronchial epithelial cells. Calu-3 cells were grown to confluency on transwell inserts as previously described (*24*). Cells were infected with Tx/91 (▲), Tx/91 HA:1918 (□), 1918 HA/NA/M/NP/NS:Tx/91 (●), or 1918 (Δ) virus at an MOI of 0.01 for 1 hour at 37°C. Unbound virus was removed by washing the cells 3 times, and infected cells were cultured in Dulbecco's modified Eagle's medium (DMEM) medium supplemented with 0.3% bovine serum albumin in the presence (**A**) or absence (**B**) of trypsin (1 μg/ml; Sigma, St. Louis, MO). Apical and basolateral (not shown) supernatants were collected at the indicated times and virus content was determined in a standard plaque assay. The values shown represent the mean virus titer of fluids from three replicate infected cultures. *The 1918 virus titers are significantly ($P < 0.05$) different from those of all other virus infection groups as determined by analysis of variance.

(Tumpey et al. 2005)

www.sciencemag.org SCIENCE VOL 310 7 OCTOBER 2005

Logistic growth kinetics

Growth rate (gr) of

- 1918 virus (0.98 *pfu/ml/h*)
- Tx/91 virus (0.73 *pfu/ml/h*)

Relative increase of the gr ~ 33%

Relative increase in the carrying capacity ~ 100-fold

Virus control: the type I IFN response against coronavirus (Murine Hepatitis Virus) liver disease in wt mice

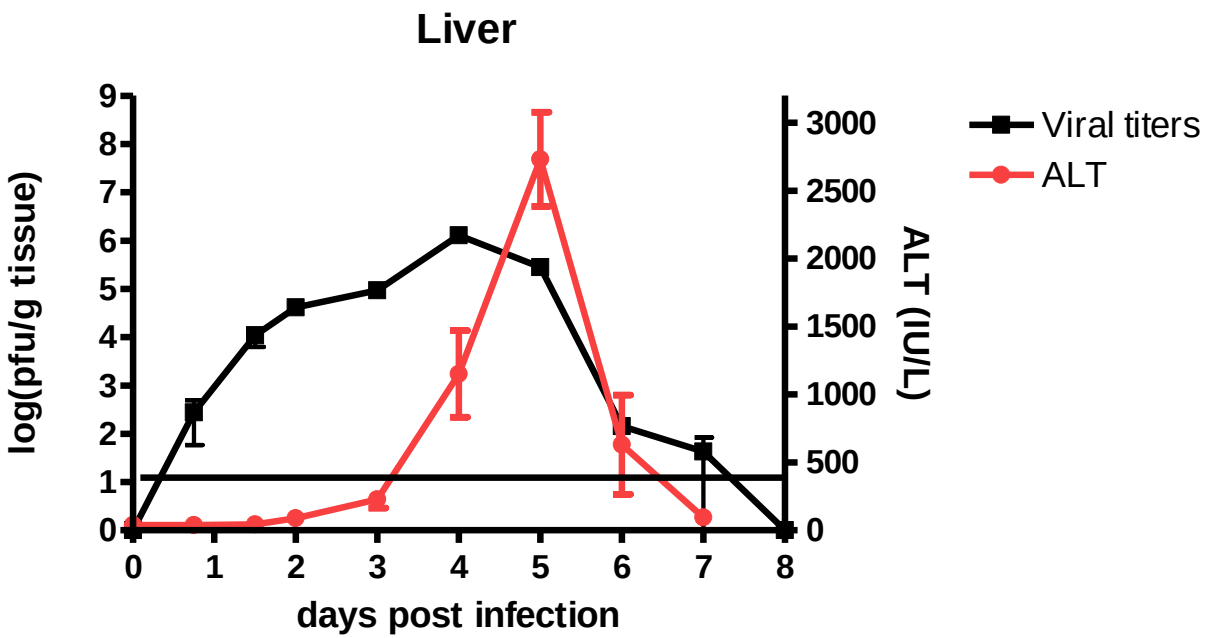

Liver enzymes and viral titers in the liver

Inverse problem -> data assimilation

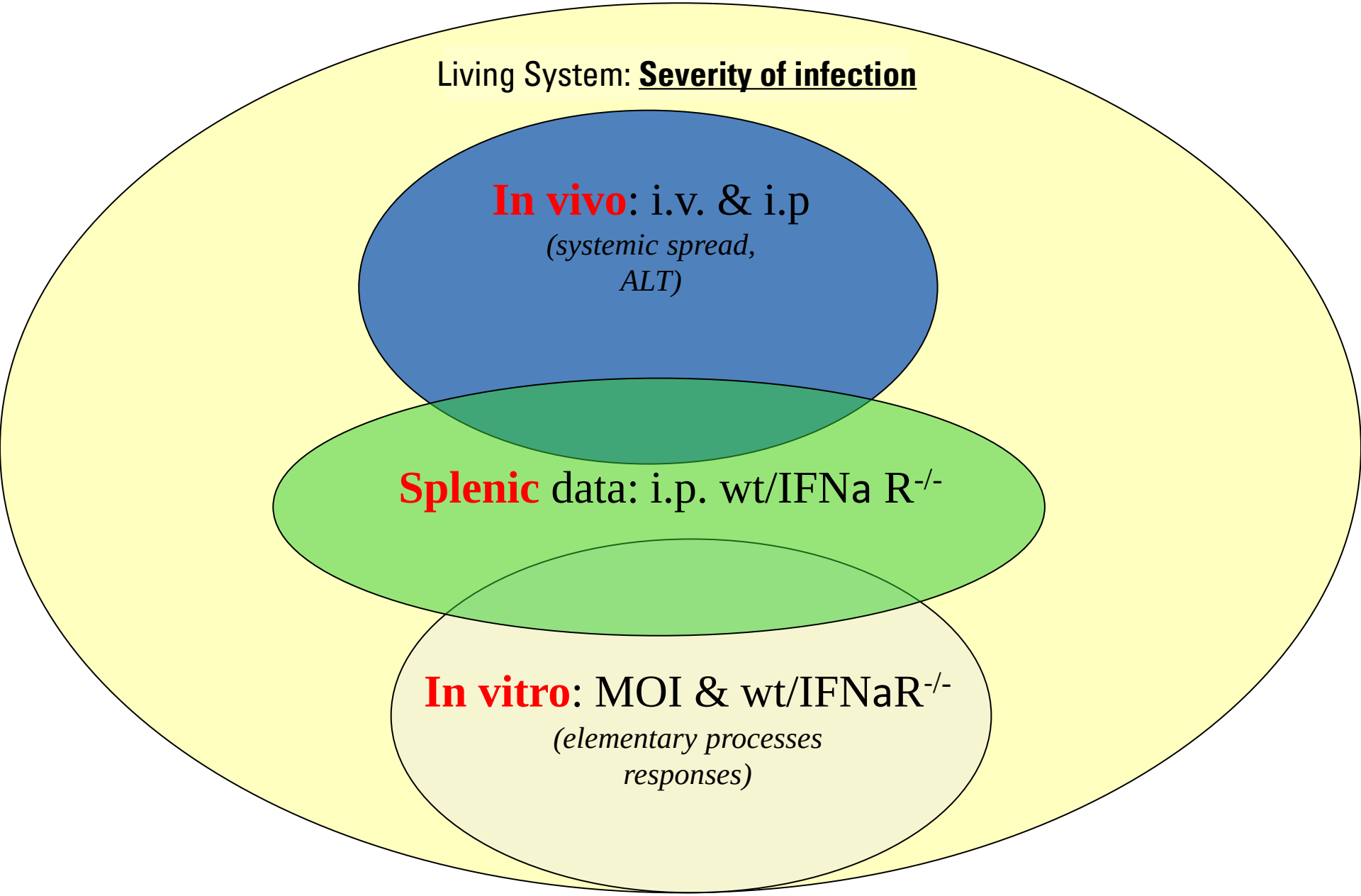

Maximum likelihood parameter estimation

$$\frac{d}{dt}\mathbf{y}(t) = \mathbf{f}\big(\mathbf{y}(t), \mathbf{y}(t-\tau), \mathbf{p}\big), \quad t \in [t_0, T], \quad \tau > 0$$

$$\mathbf{y} \in R^{n_y}, \quad \mathbf{p} \in R^{n_p}$$

$$\mathbf{y}(t) = \varphi(t), t \in [t_0 - \tau, t_0].$$

•Observation data $\{t_j, \mathbf{y}_j\}_{j=1}^{n_{obs}}$

•Likelihood function

$$\mathbf{y}_j \sim \mathcal{N}\big(\mathbf{y}(t_j), \Sigma_j\big)$$

$$\mathcal{H}\big(\mathbf{y}_j; \mathbf{p}\big) = \frac{1}{\sqrt{(2\pi)^{n_y} \det \Sigma_j}} \exp\left\{-\frac{1}{2}\big[\mathbf{y}(t_j) - \mathbf{y}_j\big]^{\mathrm{T}} \Sigma_j^{-1} \big[\mathbf{y}(t_j) - \mathbf{y}_j\big]\right\}$$

$$\mathcal{L}(\mathbf{p}) = \prod_{j=1}^{n_{obs}} \mathcal{H}\big(\mathbf{y}_j; \mathbf{p}\big)$$

$$\mathbf{p}^* = \arg\max_{\mathbf{p} \in D} \mathcal{L}\big(\mathbf{p}\big)$$

ML and Information-theoretic ranking

- the observational errors, i.e. the residuals defined as a difference between observed and model-predicted values, are normally distributed,
- the errors in observations at successive times are independent,
- the errors in the components of the state vector are independent,
- the variance of observation errors (σ^2) is the same for all the state variables and observation times.

$$\ln(\mathcal{L}(\mathbf{p};\sigma)) = -0.5\Big(n_{\mathrm{d}}\ln(2\pi) + n_{\mathrm{d}}\ln(\sigma^2) + \sigma^{-2}\Phi(\mathbf{p})\Big)$$

$$\Phi(\mathbf{p}) = \sum_{i=1}^{4}\left(\sum_{j=0}^{7}\left(N_j^i - N_j(t_i;\mathbf{p})\right)^2 + \left(D^i - D(t_i;\mathbf{p})\right)^2\right)$$

$$\partial(\ln(\mathcal{L}(\mathbf{p}^*;\sigma)))/\partial\sigma^2 = 0 \qquad \Rightarrow \qquad \sigma^{*2} = \frac{1}{n_{\mathrm{d}}}\Phi(\mathbf{p}^*)$$

Akaike measure of the distance between the given model and an 'ideal' model of the data:

$$\mu_{\mathrm{AIC}} = n_{\mathrm{d}}\ln(\Phi(\mathbf{p}^*)) + 2(L+1),$$

$$\mu_{\mathrm{cAIC}} = n_{\mathrm{d}}\ln(\Phi(\mathbf{p}^*)) + 2(L+1) + \frac{2(L+1)(L+2)}{n_{\mathrm{d}} - L - 2}$$

Uncertainty in the parameter estimates

1. Variance-covariance analysis:

$$H(\mathbf{p}) := \left\{\frac{\partial}{\partial \mathbf{p}}\right\}\left\{\frac{\partial}{\partial \mathbf{p}}\right\}^{\mathrm{T}} \Phi(\mathbf{p}) \in \mathbb{R}^{n_p \times n_p}, \quad H_{k,m}(\mathbf{p}) = \frac{\partial^2}{\partial p_k \partial p_m}\Phi(\mathbf{p}), \quad \Xi(\mathbf{p}^*) = \frac{2\Phi(\mathbf{p}^*)}{n_{\mathrm{d}} - n_p} H^{-1}(\mathbf{p}^*) \in \mathbb{R}^{n_p \times n_p},$$

$$\sigma_k = \sqrt{\Xi_{k,k}(\mathbf{p}^*)} \quad \rightarrow \quad \boxed{\mathrm{CI}_{p_k} = [p_k^* - \sigma_{p_k} z(\theta, n_f),\ p_k^* + \sigma_{p_k} z(\theta, n_f)], \quad k = 1, 2, \ldots, n_p}$$

2. Profile-likelihood-based analysis: $\boxed{[p_k^{\min},\ p_k^{\max}]}$

$$|\ln(\mathcal{L}(\tilde{\mathbf{p}})) - \ln(\mathcal{L}(\mathbf{p}^*))| \leq \frac{1}{2}\chi^2_{1,0.95} \quad \text{whenever } p_k \in [p_k^{\min},\ p_k^{\max}]$$

$$\mathcal{L}(\tilde{\mathbf{p}}) := \max_{\mathbf{p} \in S(p_k)} \mathcal{L}(\mathbf{p}), \text{ where } S(p_k) := \{[p_1, p_2, \ldots, p_{k-1}, p, p_{k+1}, \ldots, p_{n_p}]|_{p \text{ fixed}}\}$$

3. Bootstrap analysis: $CI_{p_{k,M}} = [\hat{p}_k^* - 1.96\sigma_{p_{k,M}},\ \hat{p}_k^* + 1.96\sigma_{p_{k,M}}]$

$$\hat{p}_k^* := \frac{\sum_{m=1}^{M} \tilde{p}_{k,m}^*}{M}, \quad \sigma_{p_{k,M}} = \left(\frac{\sum_{m=1}^{M} |\tilde{p}_{k,m}^* - \hat{p}_k^*|^2}{M-1}\right)^{1/2}$$

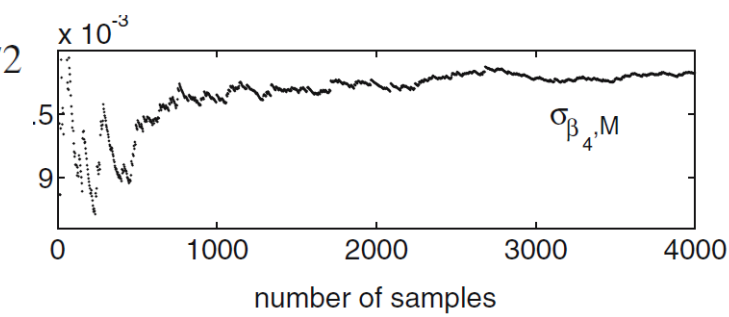

Multiscale model of MHV infection in mice

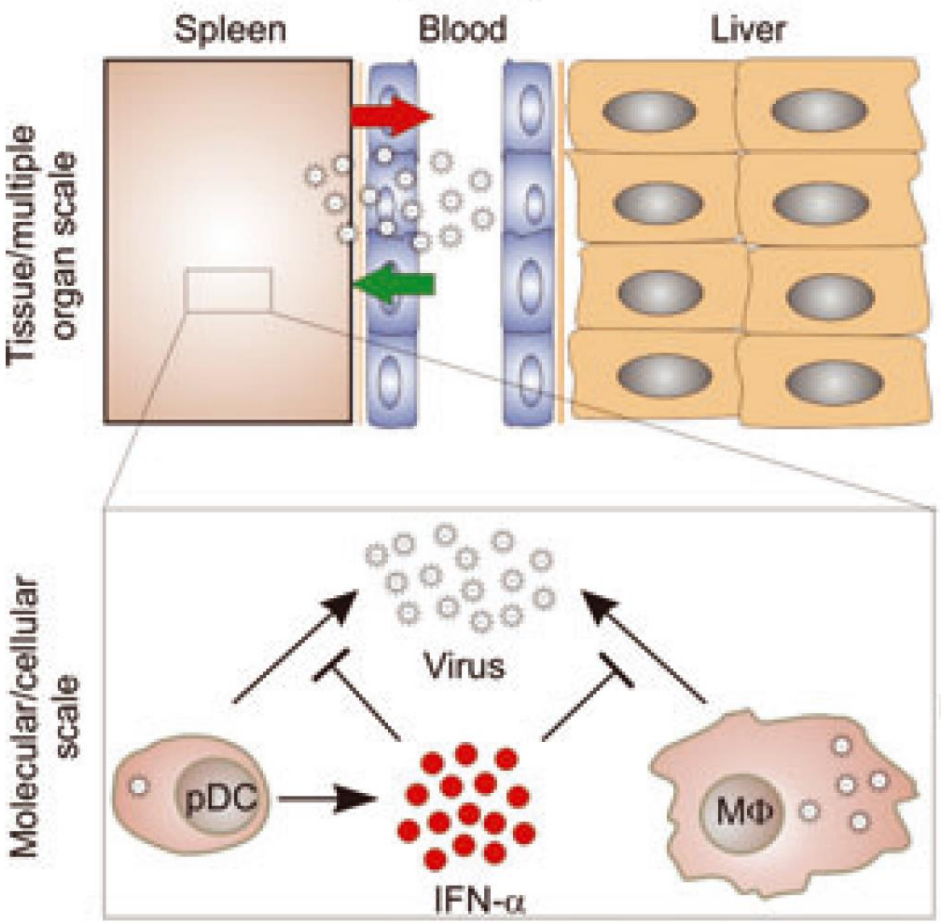

Multiple compartments

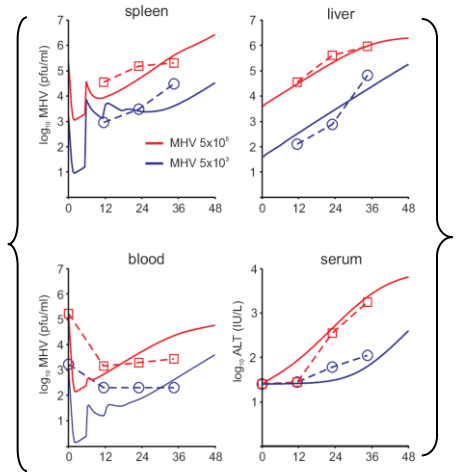

Single organ

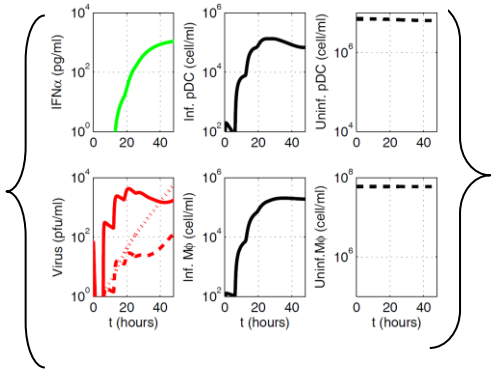

System in vitro

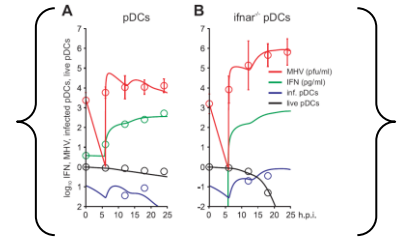

Estimated average secretion rate of type I IFN

by infected pDC ~ **15586** *molec/hr*,

by infected Macrophage ~**106** *molec/hr*

Data-driven iterative model calibration

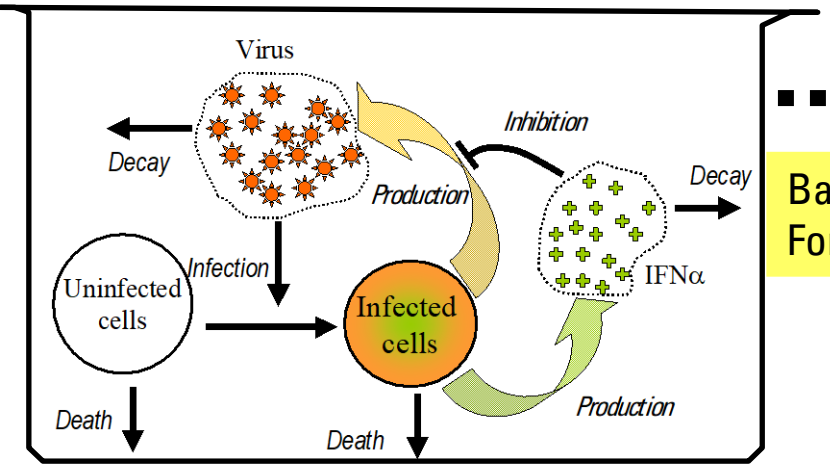

Basic Model Formulation

$$\frac{d}{dt}V(t) = \frac{\rho_V \cdot C_V(t-\tau_V)}{1+I(t)/\theta} - d_V \cdot V(t) - \sigma_V \cdot V(t) \cdot C(t)$$

$$\frac{d}{dt}I(t) = \rho_I \cdot C_V(t-\tau_I) - d_I \cdot I(t)$$

$$\frac{d}{dt}C(t) = -\sigma_V \cdot V(t) \cdot C(t) - d_C(t) \cdot C(t)$$

$$\frac{d}{dt}C_V(t) = \sigma_V \cdot C(t) \cdot V(t) - d_{CV}(t) \cdot C_V(t)$$

Parameter Identification

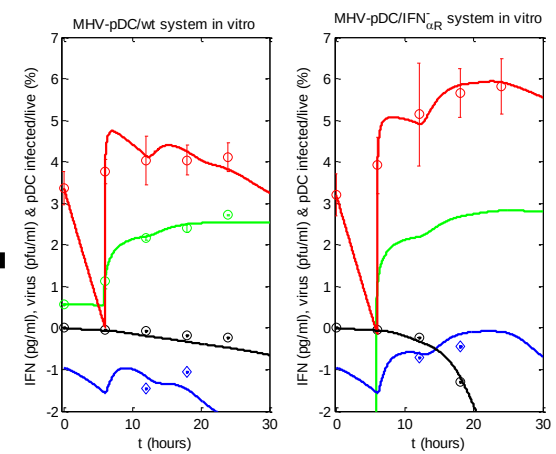

The average secretion rate of IFNa is

- for infected pDC ~ **15586** *molec/hr*,
- for infected Macrophages ~**106** *molec/hr*

Data set extension

Model parameter	pDC
Virus production rate: r_V (pfu/cell/h)	1.7
IFNa production rate: r_I (pg/cell/h)	0.0004
IFNa threshold for 50% reduction of virus production rate: q (pg/ml)	45.8
Infection rate of target cells: s_V	10^{-6}
Initial fraction of infected cells for "Multiplicity of Infection = 1" experiment: $C_V(0)$	0.1
Virus production delay: t_V (h)	6.0
IFNa production delay: t_I (h)	5.8
Gompertz death rate parameters for infected cells: d_{0C} (1/h) & k_C (1/h)	0.2 & 0.087

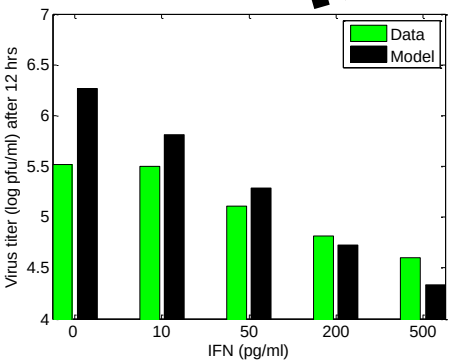

Validation

The systemic model of MHV infection & IFNa response

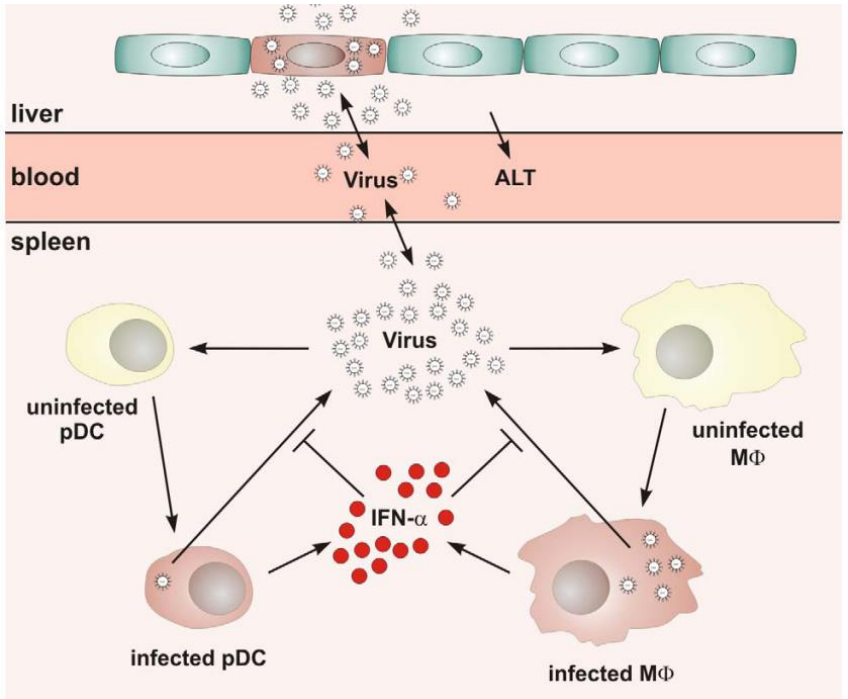

$$\frac{d}{dt}V_L(t)=\beta_L\cdot V_L(t)\cdot(1-V_L(t)/K_L)-\mu_{LB}\cdot V_L(t)$$
$$+\mu_{BL}\cdot V_B(t)\cdot Q_B/Q_L$$

$$\frac{d}{dt}V_B(t)=\mu_{LB}\cdot V_L(t)\cdot Q_L/Q_B+\mu_{SB}\cdot V_S(t)\cdot Q_S/Q_B$$
$$-(\mu_{BS}+\mu_{BL}+\mu_{BO})\cdot V_B(t)$$

$$\frac{d}{dt}A(t)=\rho_A\cdot V_L(t)+d_A\cdot(A^*-A(t))$$

$$\frac{d}{dt}V_S(t)=\frac{\rho_V^{pDC}}{1+I(t)/\theta_{pDC}}C_V^{pDC}(t-\tau_V^{pDC})$$
$$+\frac{\rho_V^{M\varphi}}{1+I(t)/\theta_{M\varphi}}C_V^{M\varphi}(t-\tau_V^{M\varphi})$$
$$-\left(\sigma_V^{pDC}\cdot C^{pDC}(t)+\sigma_V^{M\varphi}\cdot C^{M\varphi}(t)\right)\cdot V_S(t)$$
$$-d_V\cdot V_S(t)-\mu_{SB}\cdot V_S(t)+\mu_{BS}\cdot V_B(t)\cdot\frac{Q_B}{Q_S}$$

$$\frac{d}{dt}I(t)=\rho_I^{pDC}\cdot C_V^{pDC}(t-\tau_I^{pDC})+\rho_I^{M\varphi}\cdot C_V^{M\varphi}(t-\tau_I^{M\varphi})$$
$$-d_I\cdot I(t)$$

$$\frac{d}{dt}C_V^{pDC}(t)=\sigma_V^{pDC}\cdot V_S(t)\cdot C^{pDC}(t)-d_{0CV}^{pDC}\cdot C_V^{pDC}(t)$$

$$\frac{d}{dt}C_V^{M\varphi}(t)=\sigma_V^{M\varphi}\cdot V_S(t)\cdot C^{M\varphi}(t)-d_{0CV}^{M\varphi}\cdot C_V^{M\varphi}(t)$$

$$\frac{d}{dt}C^{pDC}(t)=-\sigma_V^{pDC}\cdot V_S(t)\cdot C^{pDC}(t)$$
$$+d_{0C}^{pDC}\cdot\left(C_0^{pDC}-C^{pDC}(t)\right)$$

$$\frac{d}{dt}C^{M\varphi}(t)=-\sigma_V^{M\varphi}\cdot V_S(t)\cdot C^{M\varphi}(t)$$
$$+d_{0C}^{M\varphi}\cdot\left(C_0^{M\varphi}-C^{M\varphi}(t)\right)$$

Calibrated models for MHV infection pDC и M□ □

Table 1. Best-fit parameter values for MHV infection of pDC and Mϕ

Biological parameter Notation (*units*)	**pDC Best-fit estimate**; 95% **CI**	**Mϕ Best-fit estimate**; 95% **CI**
Virus production rate, ρ_V (*pfu/cell/h*)	1.7 [0.62, 5.5]	36.7 [18, 220]
Type I IFN production rate, ρ_I (*pg/cell/h*)	4.4×10^{-4} [1.3×10^{-4}, 1.6×10^{-3}]	$3.0\times10^{-6}/1.0\times10^{-6}$ (*) [1.2×10^{-6}, 1.9×10^{-5}]
The threshold for 50% reduction of virus production rate by type I IFN, θ (*pg/ml*)	45.8 [26, 80] [endogenous IFN]	0.09/0.97 (**) [0.007, 0.7] [endogenous IFN]
Infection rate of target cells, σ_V (*cell/pfu/h*)	1.3×10^{-6} [7.0×10^{-7}, 2.8×10^{-6}]	$5.4\times10^{-6}/0.9\times10^{-7}$ (***) [1.7×10^{-6}, $> 10^{-4}$]
Initial fraction of infected cells for "Multiplicity of Infection = 1" experiment: $C_V(0)$	0.11 [0.029, 0.26]	1.0
Virus production delay, τ_V (*h*)	5.96 [5.88, 5.98]	5.99 [5.98, 6.0]
Type I IFN production delay, τ_I (*h*)	5.77 [5.22, 5.93]	5.8
Gompertz death rate parameters for infected cells, d_{0CV} (*1/h*) & k_{CV} (*1/h*)	0.2 & 0.087 [0.015, 6.0] & [0.029, 0.19]	0.049 & 0.057 [0.024, 0.11] & [0.012, 0.1

(*) Refined by in vivo data
(**) Refined by data (Eriksson et al. 2008)
(***) Refined by in vivo data

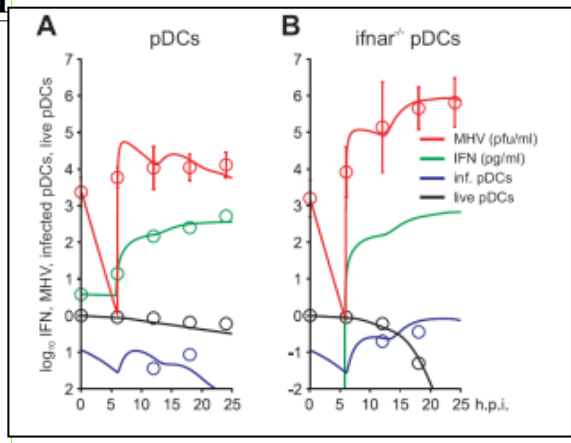

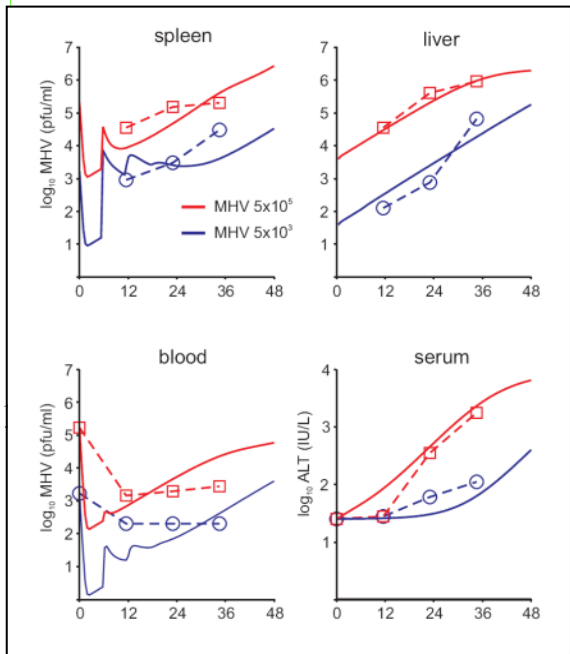

Чувствительность индекса тяжести заболевания к скорости репликации вирусов в различных органах

Тропизм к клеткам в селезенке

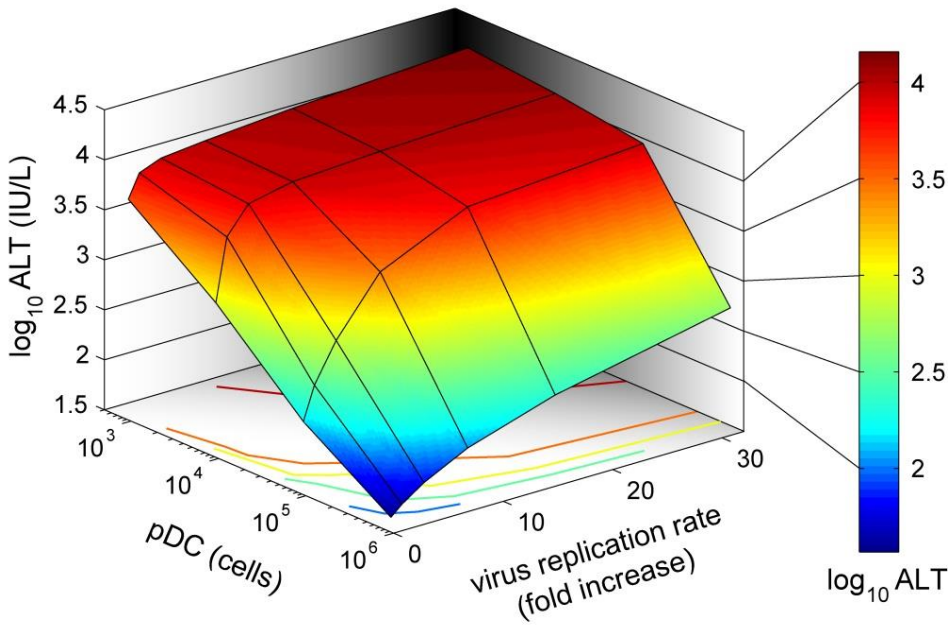

Робастная защита организма: 30-кратная интенсификация репликации вирусов в <u>лимфоидных органах</u>

Тропизм к клеткам печени

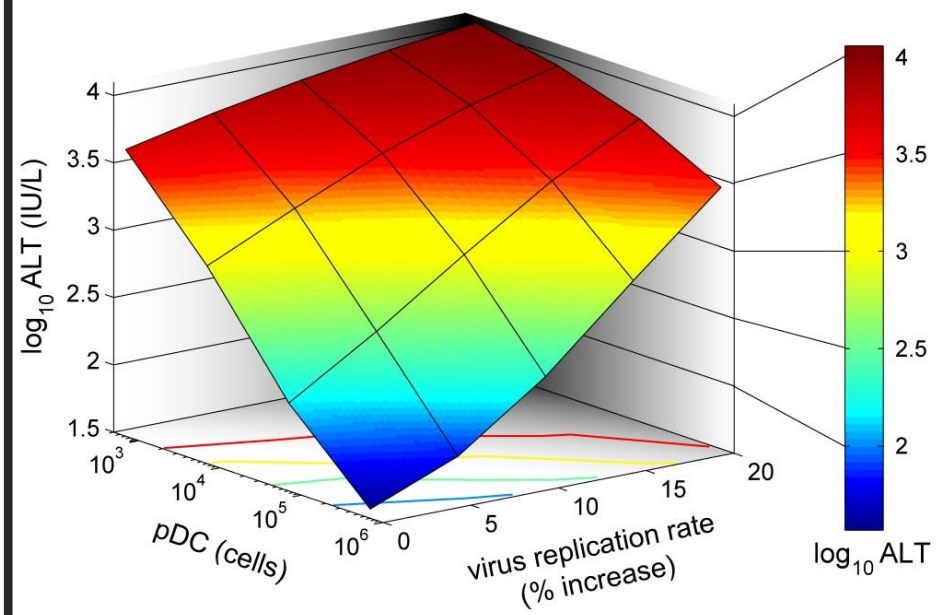

Уязвимость защиты организма: 15% интенсификация репликации вирусов в <u>периферических органах</u> приводит к тяжелой инфекции

Outline

Исследование робастности защиты системой интерферона при коронавирусной инфекции мышей.

Идентификация новых мишеней для противовирусной терапии ВИЧ-1.

Olga Shcherbatova

Предсказание терапевтического эффекта блокады рецептора PD-1 в хроническую фазу ВИЧ-1 инфекции.

Исследование влияния подвижности Т-лимфоцитов в лимфатическом узле на эффективность элиминации зараженных клеток при ВИЧ-1 инфекции.

Геометрическое моделирование структурно-функциональной организации лимфатических узлов.

Multiscale processes underlying HIV infection

Andreas Meyerhans

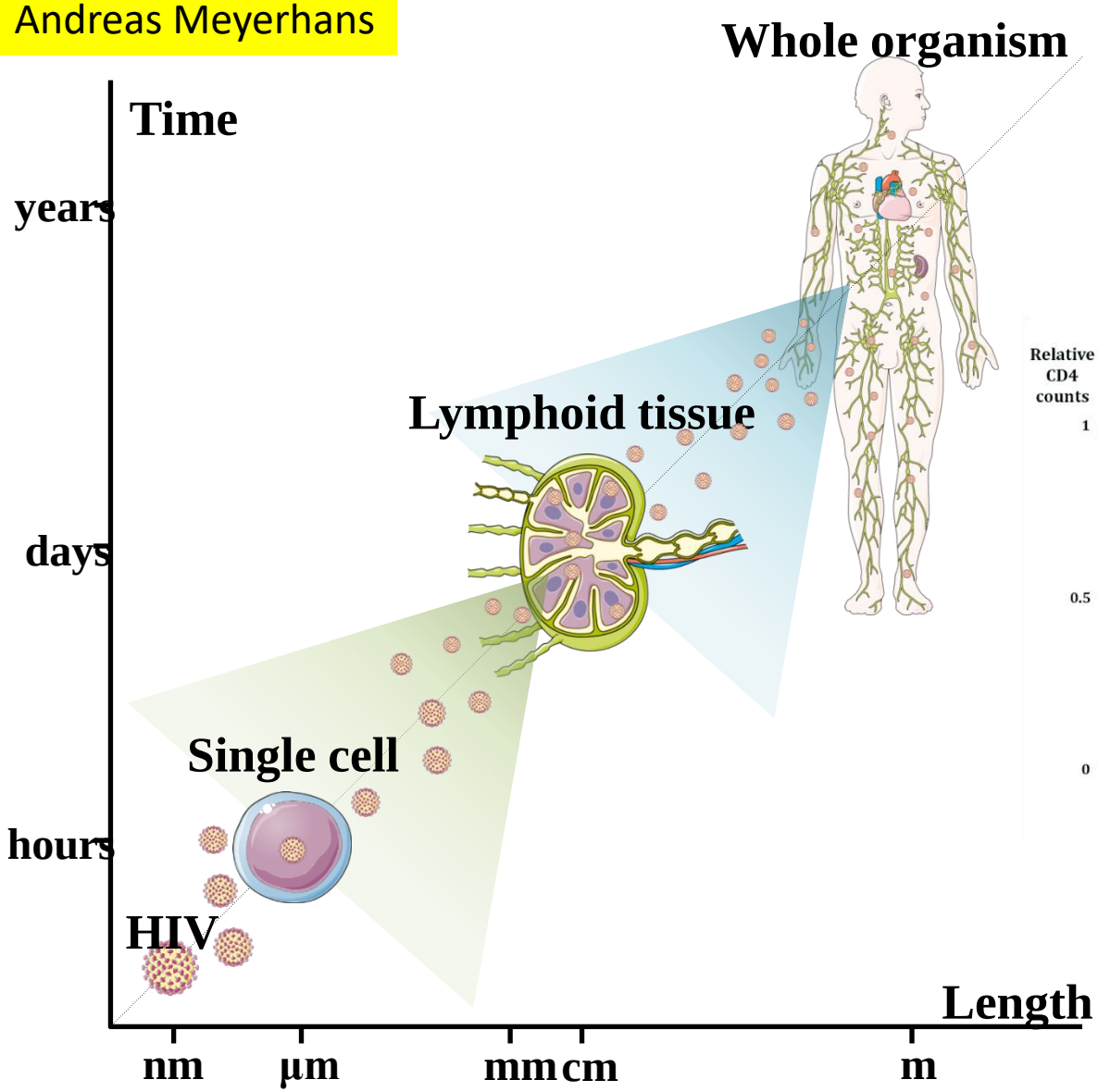

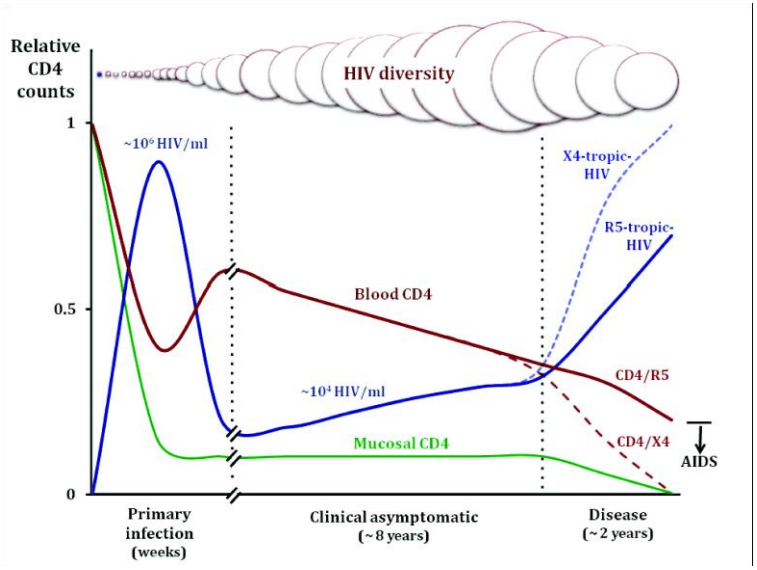

G. Bocharov, et al. Human Immunodeciency Virus Infection: from Biological Observations to Mechanistic Mathematical Modelling

Math. Model. Nat. Phenom. Vol. 7, No. 5, 2012, 78-104

Biochemical scheme of HIV-1 replication cycle

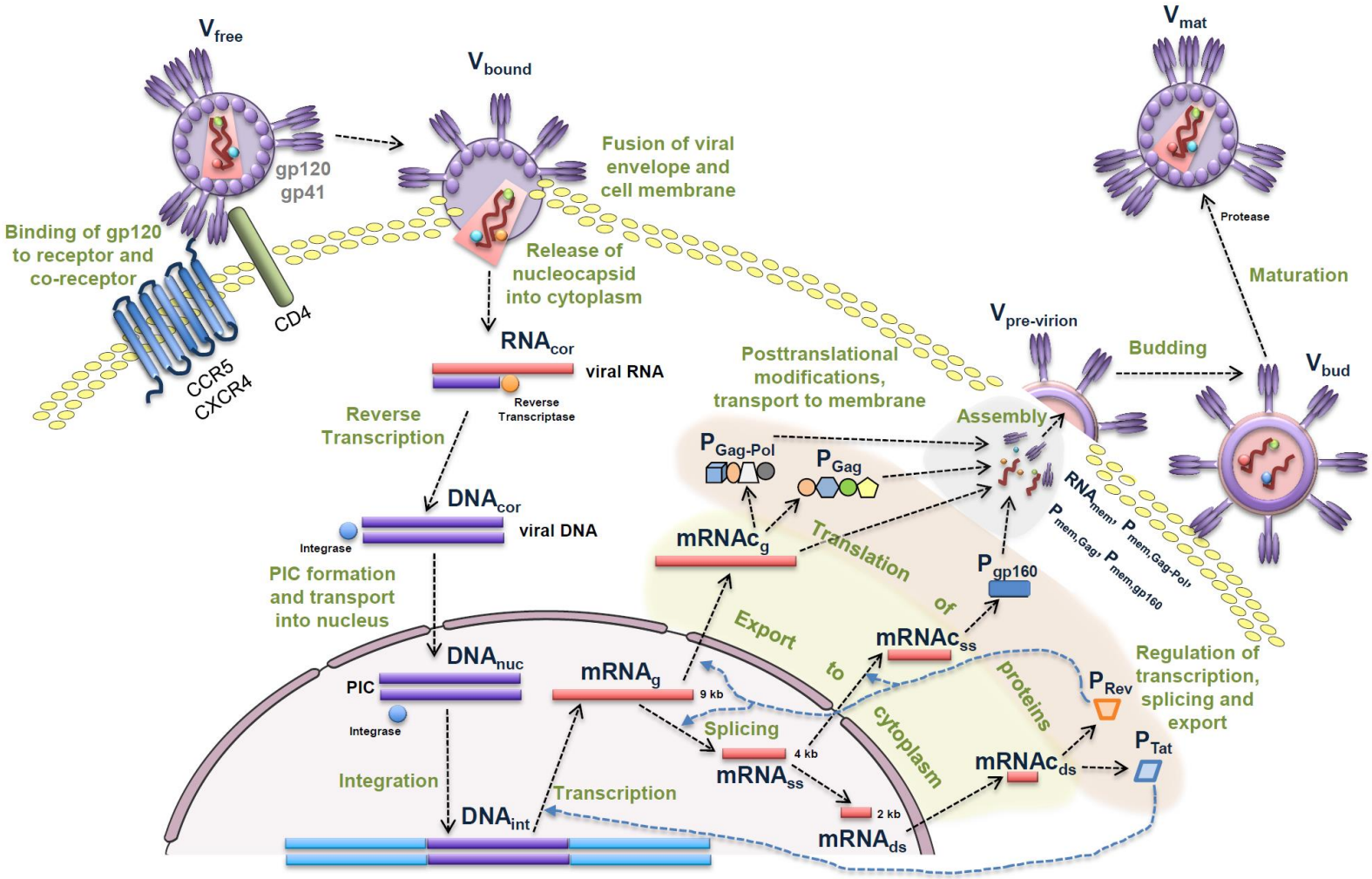

Pathogens **2020**, *9*, 255; doi:10.3390/pathogens9040255

Calibrated model of HIV-1 replication in activated CD4 T cells

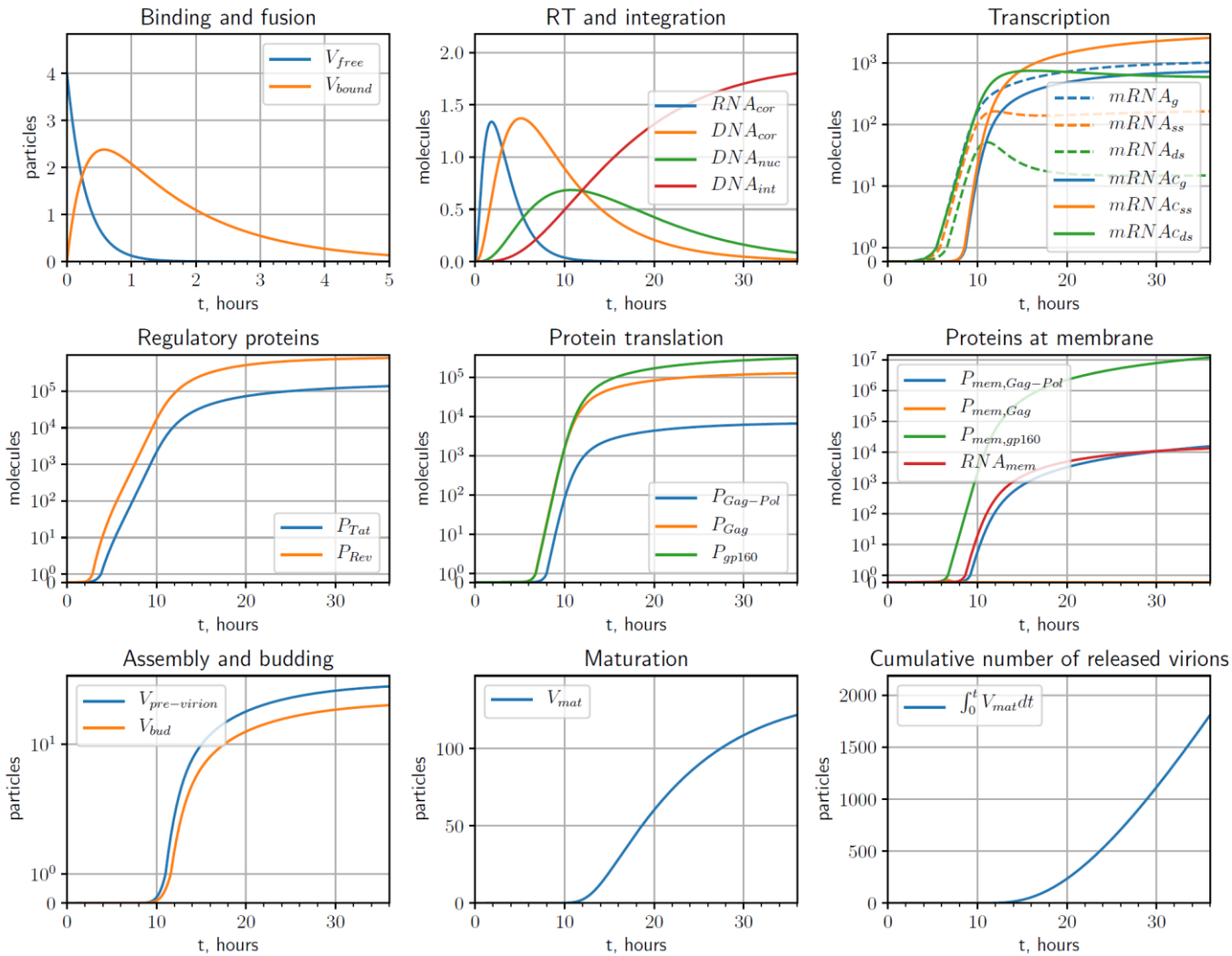

Pathogens **2020**, *9*, 255; doi:10.3390/pathogens9040255

Normalized sensitivity to process parameters

$$\frac{d}{dt}\boldsymbol{y}(t) = \boldsymbol{f}(t, \boldsymbol{y}(t), \boldsymbol{p}),\ t \in [t_0, T]$$

$$\boldsymbol{y}(t) = \phi(t, \boldsymbol{p}),\ t = t_0$$

$$J(\boldsymbol{y}) = \int_0^T V_{mat} dt$$

$$-\frac{d\boldsymbol{w}(t)}{dt} - \left[\frac{\partial \boldsymbol{f}}{\partial \boldsymbol{y}}\right]^T \boldsymbol{w} = \boldsymbol{e_1},\ t \in [t_0, T]$$

$$\boldsymbol{w} = 0,\ t = T$$

$$\boldsymbol{e_1} = (0, 0, \ldots 0, 1)^T$$

$$\frac{d}{dt}\left(\frac{\partial J}{\partial p_i}\right) = \left\langle \boldsymbol{w}(t), \frac{\partial \boldsymbol{f}(t)}{\partial p_i}\delta p_i \right\rangle,\ t \in [0, T],\ \left.\frac{\partial J}{\partial p_i}\right|_0 = 0.$$

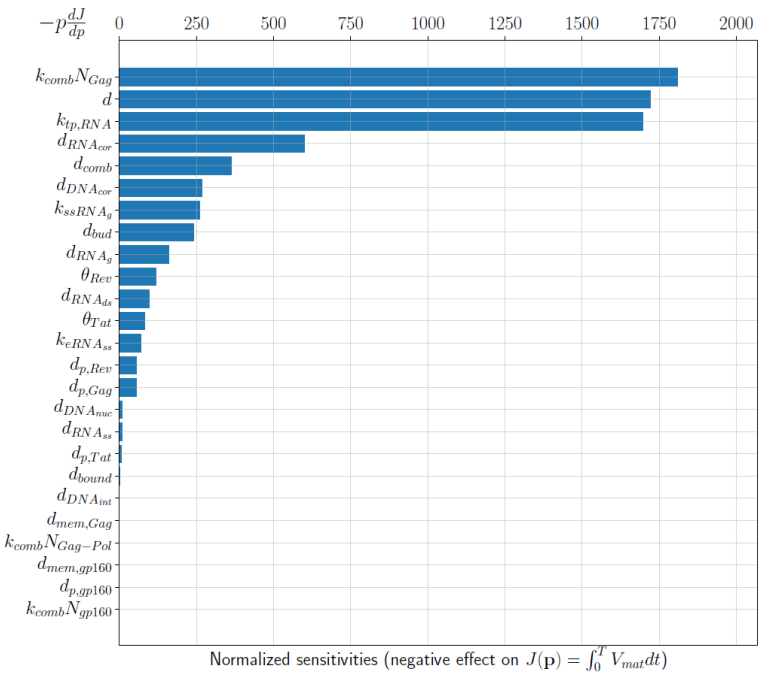

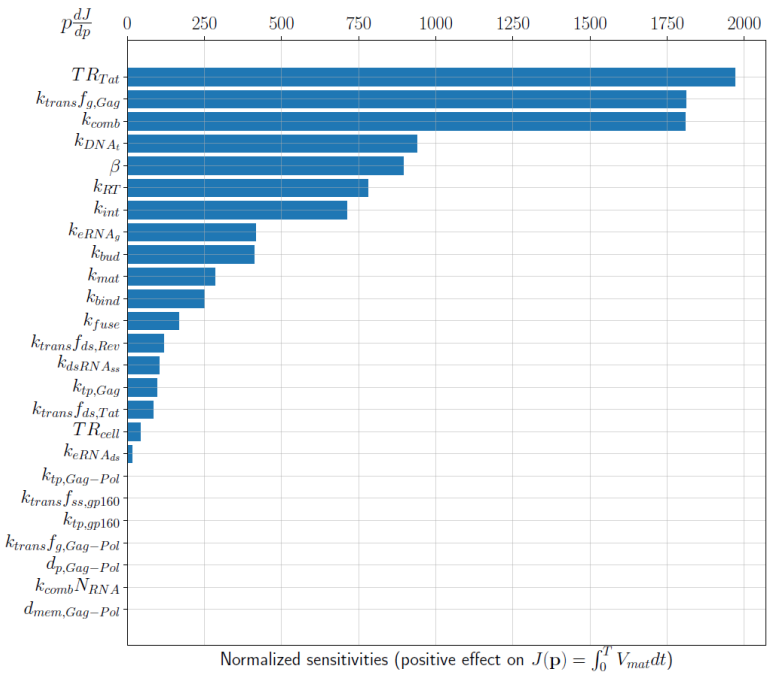

Pathogens **2020**, *9*, 255; doi:10.3390/pathogens9040255

Processes showing the strongest impact on net virus production

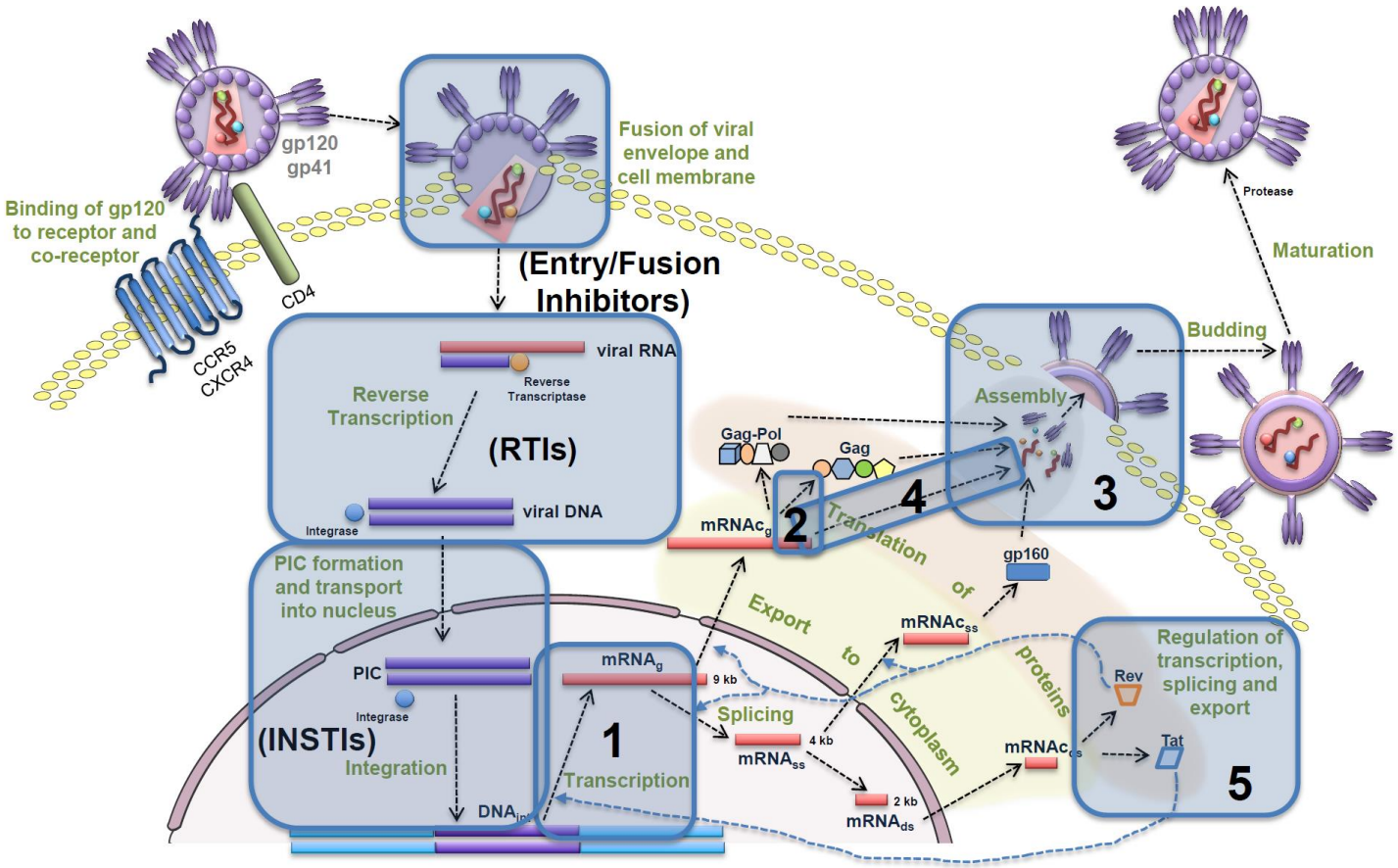

dependence on Gag and Tat-Rev regulation of HIV-1 assembly

Pathogens **2020**, *9*, 255; doi:10.3390/pathogens9040255

Outline

Исследование робастности защиты системой интерферона при коронавирусной инфекции мышей.

Идентификация новых мишеней для противовирусной терапии ВИЧ-1.

Предсказание терапевтического эффекта блокады рецептора PD-1 в хроническую фазу ВИЧ-1 инфекции. Valerya Zheltkova

Исследование влияния подвижности Т-лимфоцитов в лимфатическом узле на эффективность элиминации зараженных клеток при ВИЧ-1 инфекции.

Геометрическое моделирование структурно-функциональной организации лимфатических узлов.

Phenotypic diversity of HIV infection dynamics

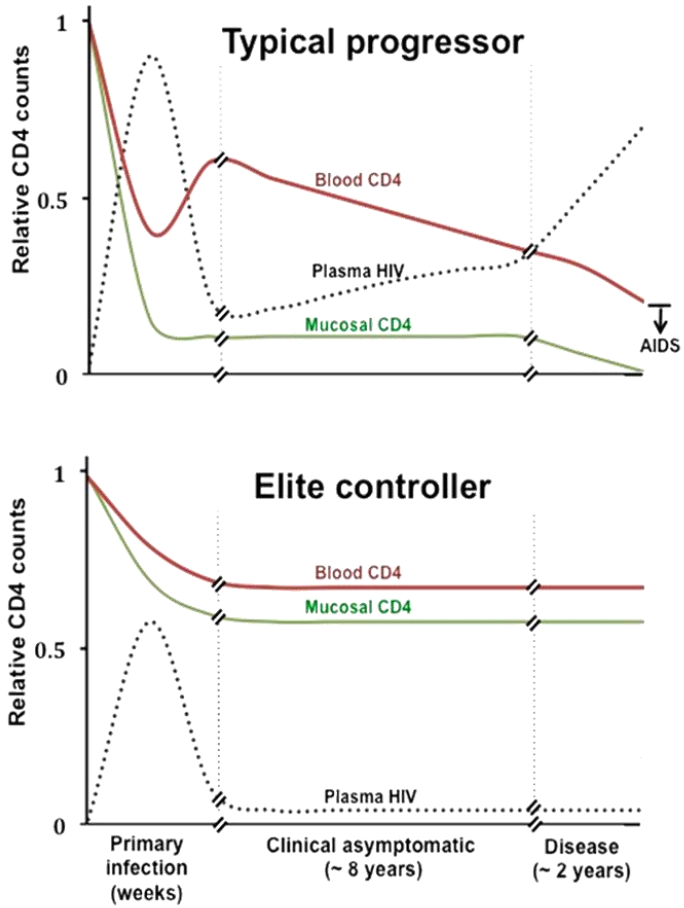

P-HVL - **progressors** (CD4+ T lymphocytes <200/ μl blood in chronic phase), high viral load (>10000 copies/ml blood in chronic phase)

P-MVL - **progressors**, medium viral load (>2000 copies/ml blood in chronic phase)

P-VC - **progressors**, viral controllers (<400 copies/ml blood in chronic phase)

SP-VC - **slow** progressors (CD4+ T lymphocytes 200-500/μl blood in chronic phase), viral controllers

SP-HIC - **slow** progressors, HIV controllers (HIV undetectable)

LTNP-HIC - **long-term nonprogressors** (CD4+ T lymphocytes > 500/μl blood in chronic phase), HIV controllers

Revitalization of exhausted lymphocytes in HIV

- Multifactorial regulation of distinct phenotypic states of lymphocytes
- The state of functional exhaustion – PD1 receptor dependent

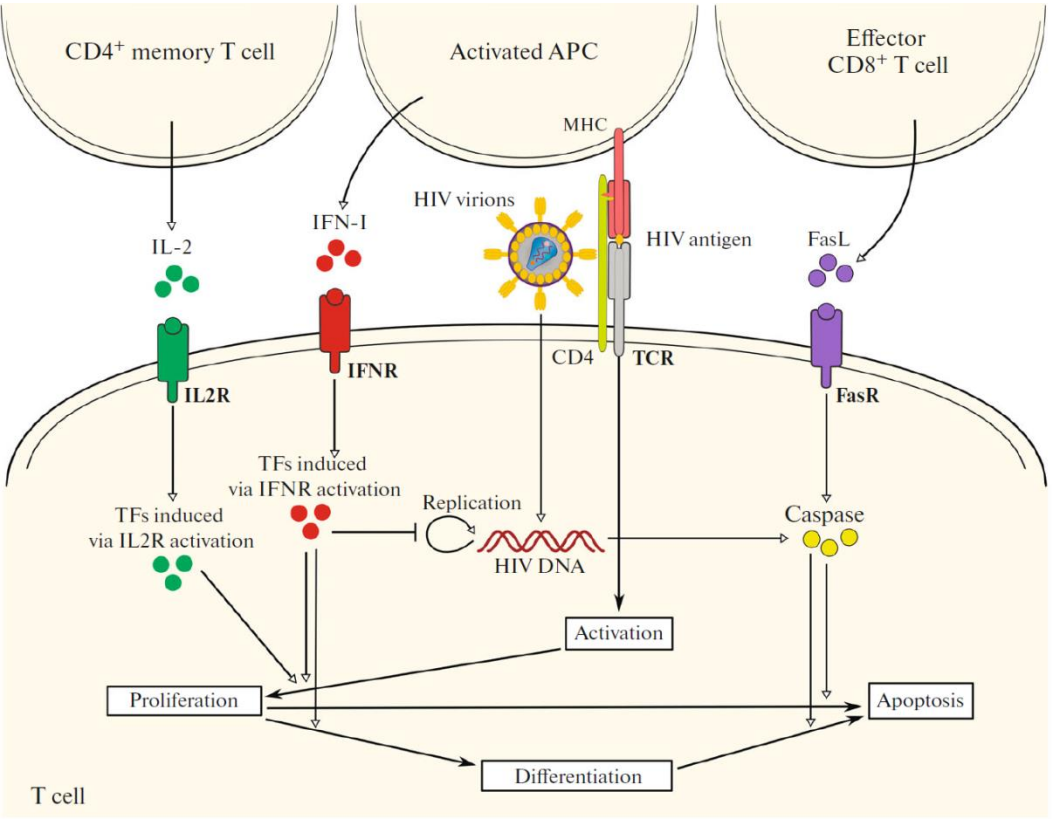

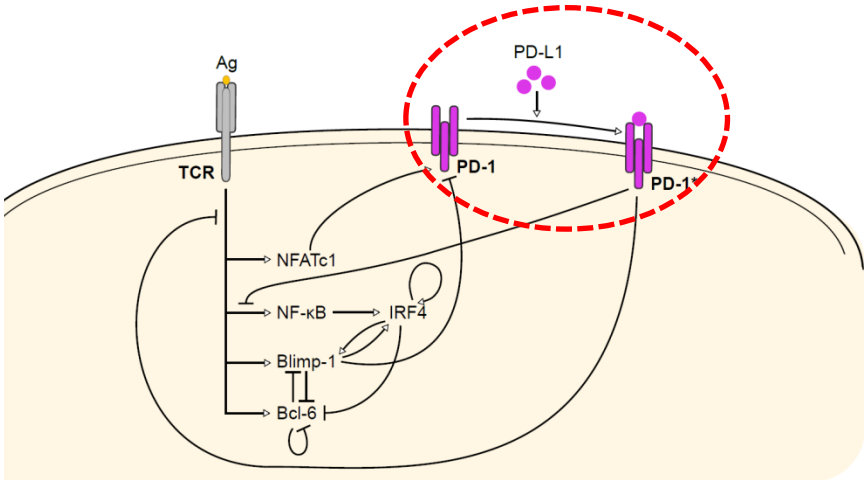

Grebennikov et al.. Molecular Biology, 2019

Question-driven data-based analysis of various components of HIV infection control

Efficacy of immunomodulatory treatment of HIV infection: phenotype-specific prediction of the CD4 T cell gain and reduction of viral load by the blockade of PD-L1 on lymphocytes

Towards personalized immunotherapy

PD1/PDL1 blockade affects

- CD8 T cells,
- CD4 T cells incl. regulatory T cells,
- B cells

Model-based layering approach to dissection of the impact of the blockade suggest that

CFSE-labelled proliferation of HIV gag-specific CD8 T cells under PD-L1 blockade

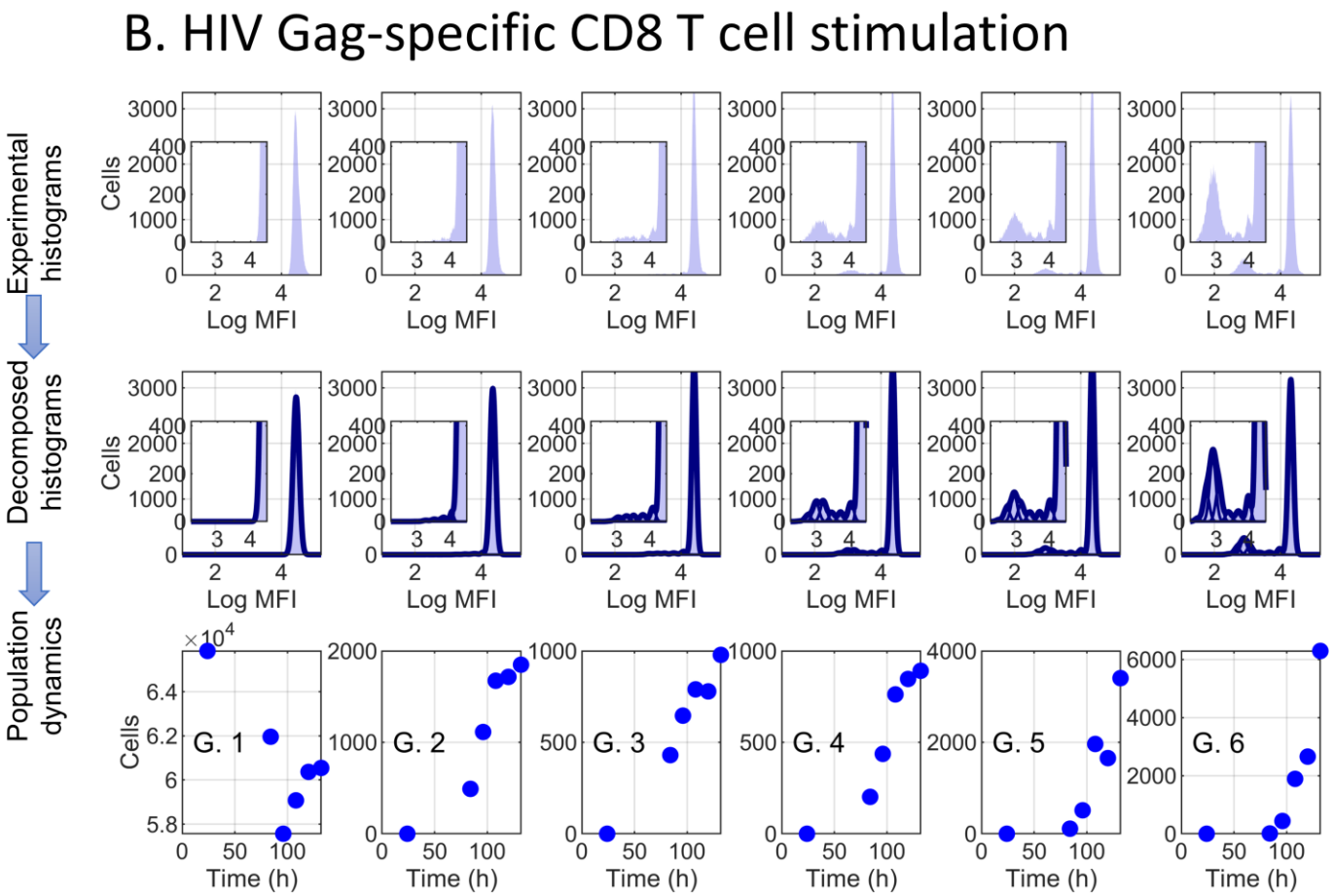

Prediction of PD-L1 inhibition effects
for HIV-infected individuals, V. Zheltkova et al. *PLOS CB* (2019)

Understanding the phenotype-specific response of HIV infected to PD-L1 blockade: who will be the beneficiary?

Study design

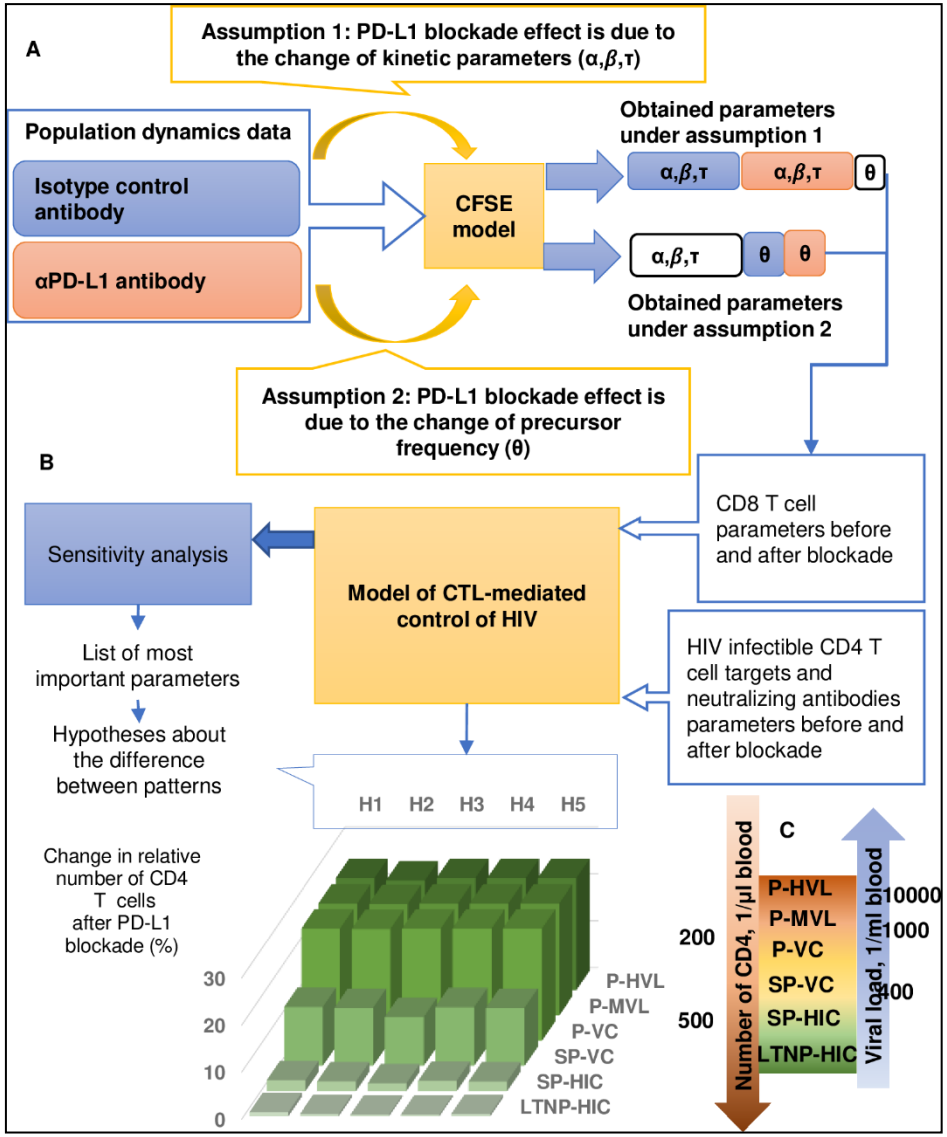

Prediction of PD-L1 inhibition effects for HIV-infected individuals, V. Zheltkova et al. *PLOS CB* (2019)

Scheme of the model of CTL-mediated HIV control

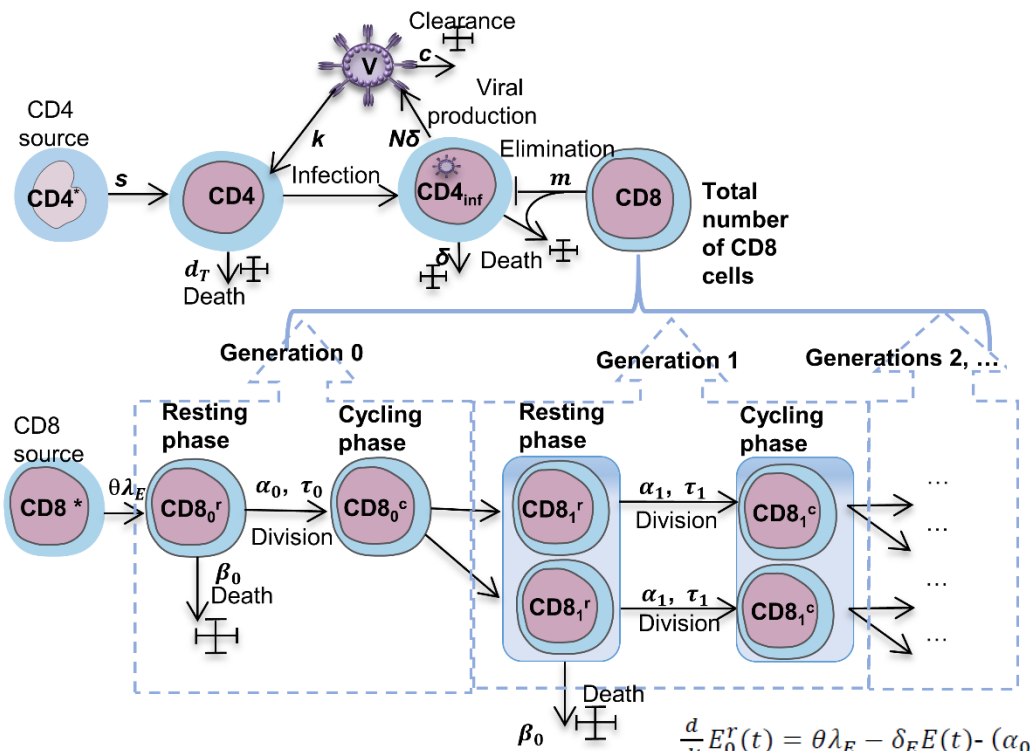

$$\frac{d}{dt}T(t) = s - d_T T - kV(t)T(t)$$

$$\frac{d}{dt}I(t) = kV(t)T(t) - \delta I(t) - mE(t)I(t),$$

$$\frac{d}{dt}V(t) = N\delta I(t) - cV(t) - kV(t)T(t),$$

$$\frac{d}{dt}E(t) = \lambda_E + \left(\frac{b_E I(t)}{k_b + I(t)} - \frac{d_E I(t)}{k_d + I(t)}\right)E(t) - \delta_E E(t)$$

$$\frac{d}{dt}E_0^r(t) = \theta\lambda_E - \delta_E E(t) - (\alpha_0 + \beta_0)E_0^r(t), \quad E_i^r(s) = 0,\ s \in [-\tau_i, 0),\ E_i^r(0) = \theta E_0;$$

$$\frac{d}{dt}E_i^r(t) = -(\alpha_i + \beta_i)E_i^r(t) + 2\alpha_{i-1}E_{i-1}^r(t - \tau_{i-1}), \quad E_{i-1}^r(s) = 0,\ s \in [-\tau_i, 0],\ i = 1, \ldots, I_{max}$$

$$\frac{d}{dt}E_i^c(t) = \alpha_i(E_i^r(t) - E_i^r(t - \tau_i)), \quad E_i^c(s) = 0,\ s \in [-\tau_i, 0],\ i = 1, \ldots, I_{max}$$

with $I_{max} = 5$.

Prediction of PD-L1 inhibition effects [1]
for HIV-infected individuals, V. Zheltkova et al. *PLOS CB* (2019)

Estimated doubling times and precursor frequencies of CD8 T cell growth after PD-L1 blockade

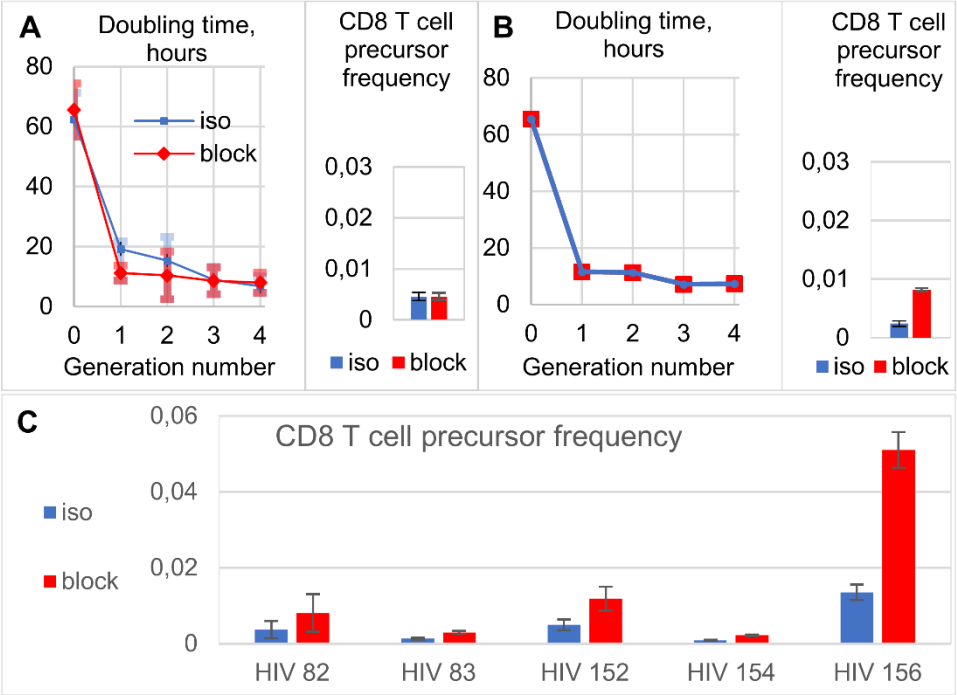

Prediction of PD-L1 inhibition effects
for HIV-infected individuals, V. Zheltkova et al. *PLOS CB* (2019

Sensitivity analysis for linking infection phenotype and the model parameters

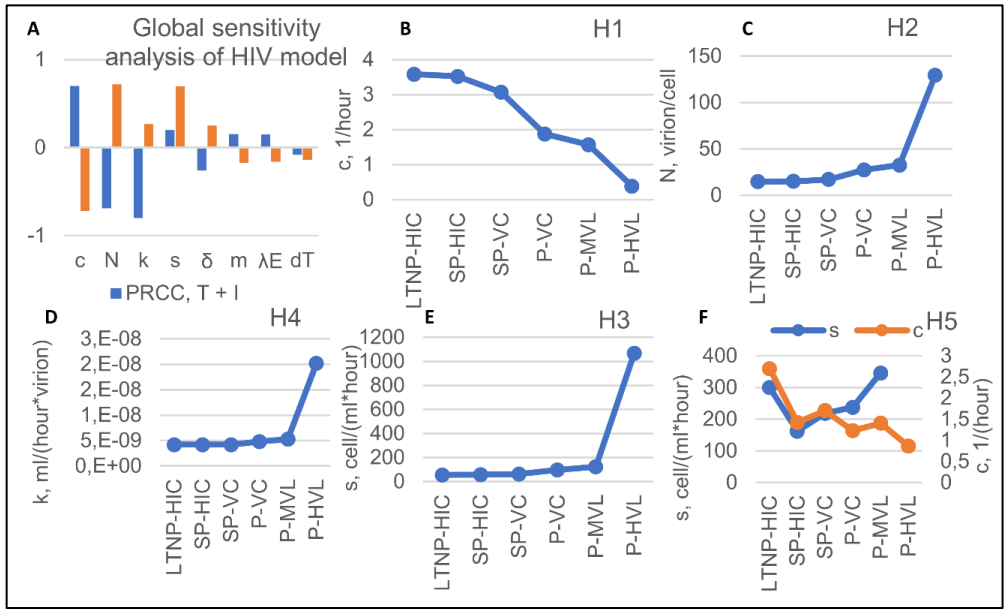

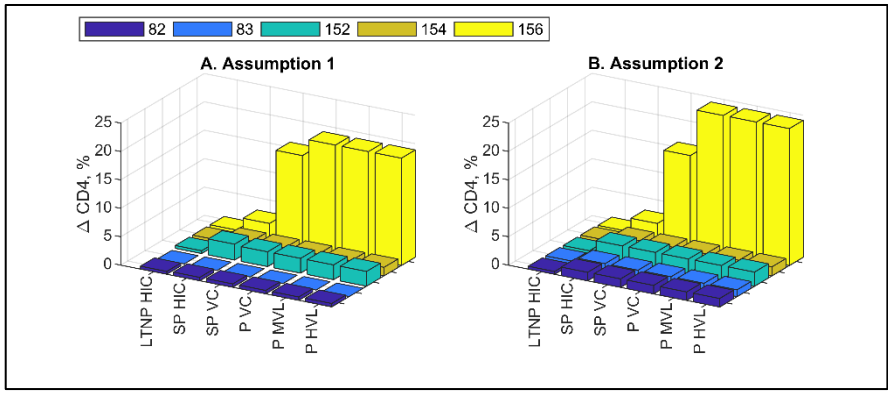

Prediction of PD-L1 inhibition effects
for HIV-infected individuals, V. Zheltkova et al. *PLOS CB* (2019)

Net effect of PD-L1 blockade on HIV load & CD4 T cell number

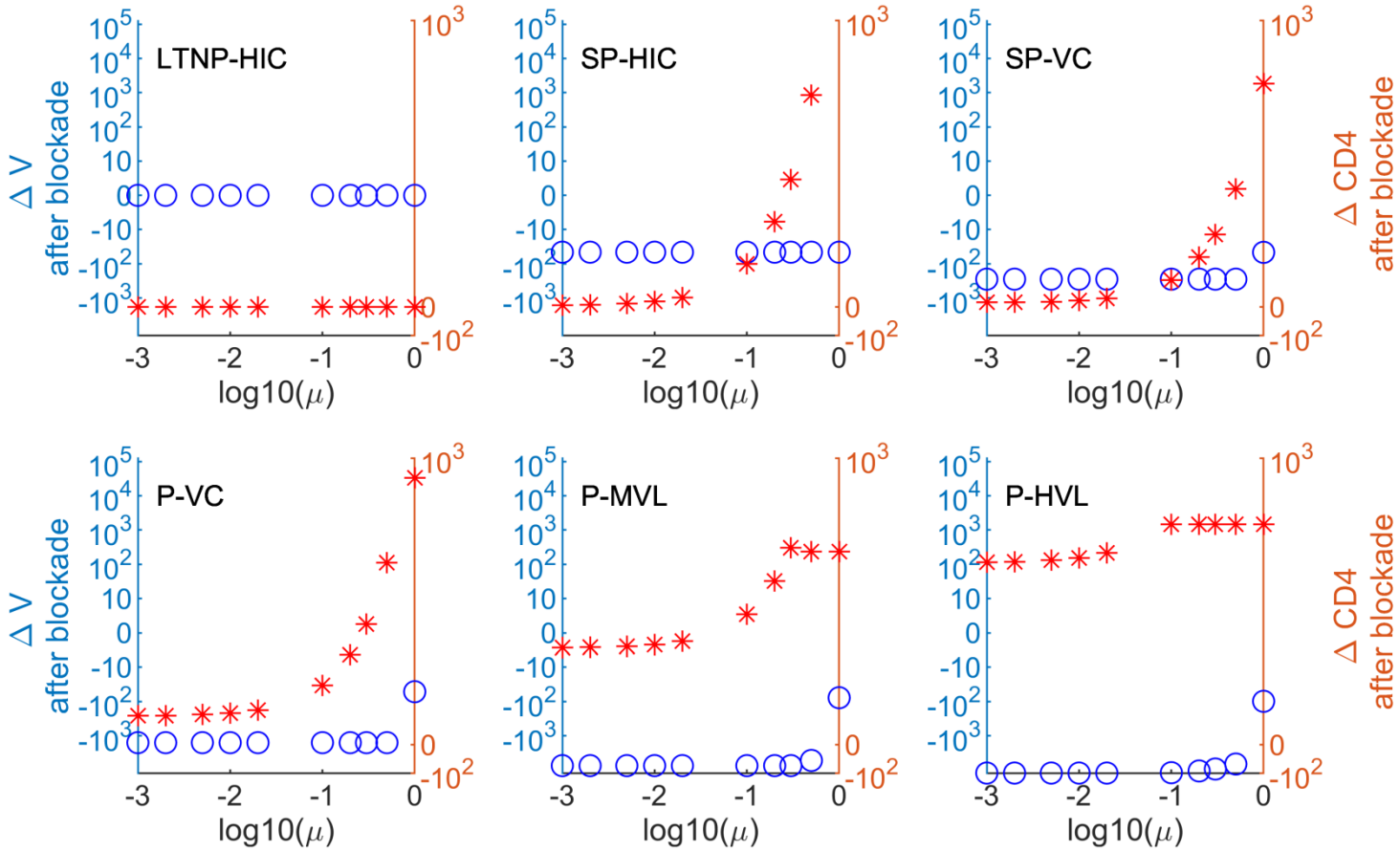

Prediction of PD-L1 inhibition effects [1]
for HIV-infected individuals, V. Zheltkova et al. *PLOS CB* (2019)

Predictions

The **net effect of PD-L1 blockade** on HIV load & CD4 T cell number

- depends on the interplay between “+” and “-” effects of CD4, CD8 and B cell lymphocyte activation
- for a physiologically relevant range of the affected model parameters, is likely to be overall beneficial

Outline

Исследование робастности защиты системой интерферона при коронавирусной инфекции мышей.

Идентификация новых мишеней для противовирусной терапии ВИЧ-1.

Предсказание терапевтического эффекта блокады рецептора PD-1 в хроническую фазу ВИЧ-1 инфекции.

Исследование влияния подвижности Т-лимфоцитов в лимфатическом узле на эффективность элиминации зараженных клеток при ВИЧ-1 инфекции.

Dmitry Grebennikov et al., 2019

Геометрическое моделирование структурно-функциональной организации лимфатических узлов.

Question-driven predictions for HIV infection control

Requirements for HIV-specific CD8 T lymphocyte motility and density on virus replication control

Dmitry Grebennikov et al., 2019

Dynamics of the individual steps of HIV life cycle

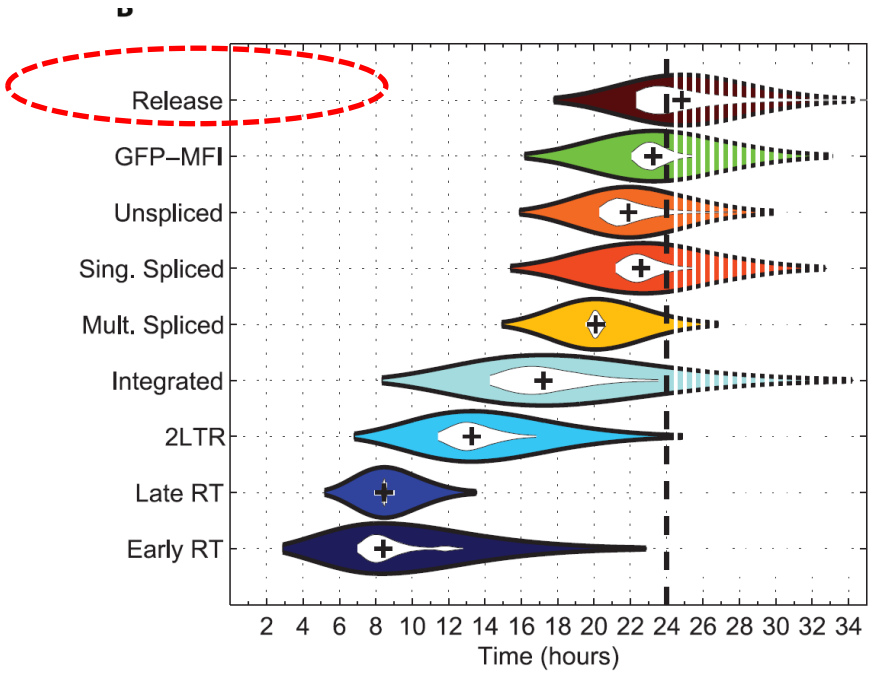

OPEN ACCESS Freely available online PLOS | PATHOGENS

24 Hours in the Life of HIV-1 in a T Cell Line 2013

Pejman Mohammadi[1,2], Sébastien Desfarges[3], István Bartha[3], Beda Joos[4], Nadine Zangger[2,3], Miguel Muñoz[3], Huldrych F. Günthard[4], Niko Beerenwinkel[1,2]*, Amalio Telenti[3,5]*, Angela Ciuffi[3,5]*

Scanning of the paracortical T cell zone for target cell expressing cognate antigen

frontiers in Immunology
ORIGINAL RESEARCH
published: 11 June 2019
doi: 10.3389/fimmu.2019.01213

Spatial Lymphocyte Dynamics in Lymph Nodes Predicts the Cytotoxic T Cell Frequency Needed for HIV Infection Control

Dmitry Grebennikov[1,2,3*], Anass Bouchnita[4], Vitaly Volpert[5,6,8], Nikolay Bessonov[7], Andreas Meyerhans[8,9] and Gennady Bocharov[2,10*]

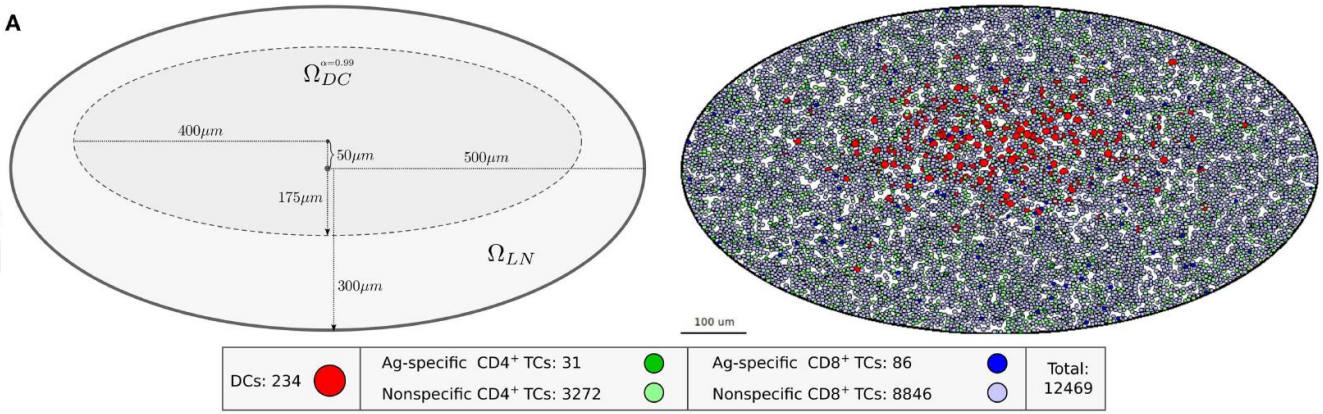

T cell motility in T cell zone of lymph nodes

A)

$$m_i \ddot{\mathbf{x}}_\mathbf{i} = \mathbf{F}_\mathbf{i}^{\mathbf{int}} + \mathbf{f}_\mathbf{i}^{\mathbf{mot}} + \mathbf{f}_\mathbf{i}^{\mathbf{dis}} = \sum_{j \neq i} \mathbf{f}_\mathbf{ij}^{\mathbf{int}} + \mathbf{f}_\mathbf{i}^{\mathbf{mot}} - \mu \dot{\mathbf{x}}_\mathbf{i}$$

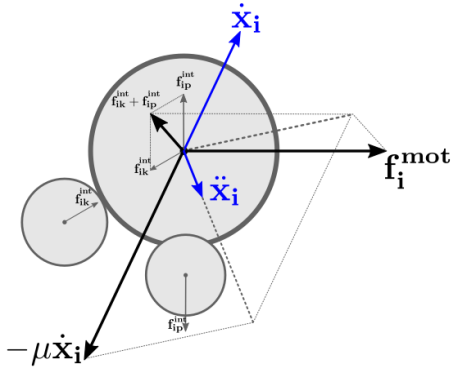

B)

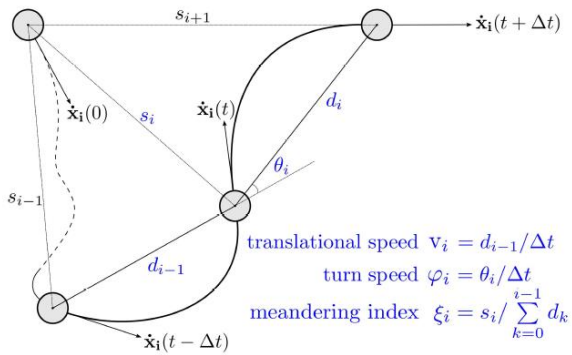

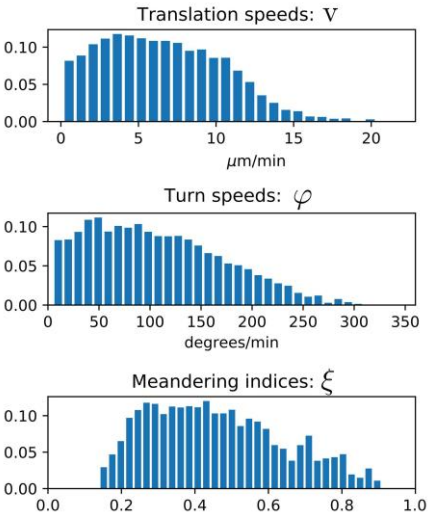

C)

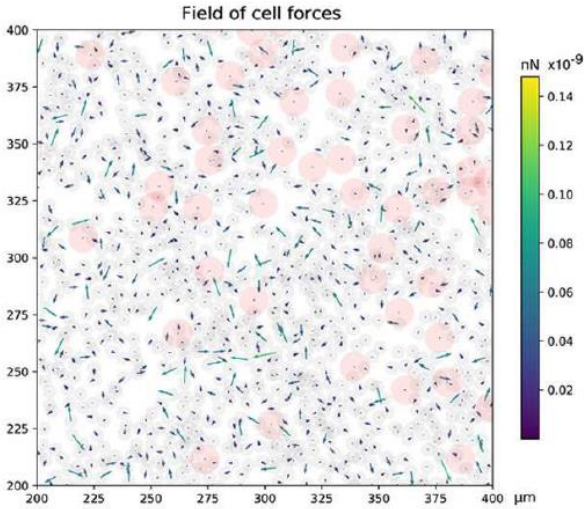

D)

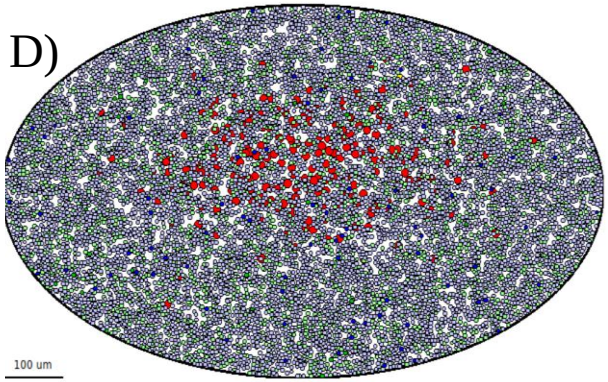

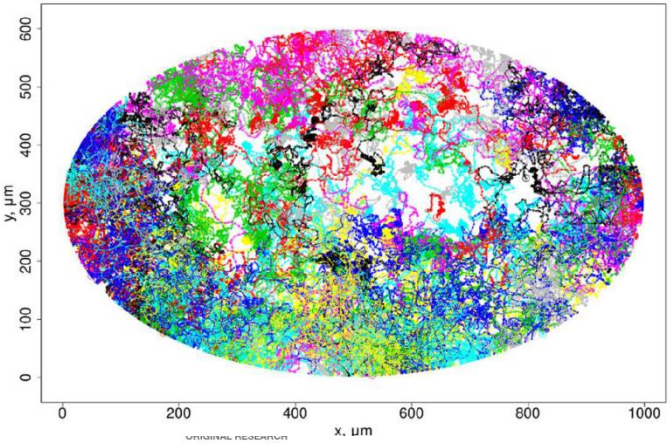

frontiers in Immunology
published: 11 June 2019
doi: 10.3389/fimmu.2019.01213

Spatial Lymphocyte Dynamics in Lymph Nodes Predicts the Cytotoxic T Cell Frequency Needed for HIV Infection Control

Dmitry Grebennikov[1,2,3], Anass Bouchnita[4], Vitaly Volpert[3,5,6], Nikolay Bessonov[7], Andreas Meyerhans[8,9] and Gennady Bocharov[2,10*]*

CTL frequency needed to stop the local HIV infection spreading within 18 hours

Basal motility

Reduced motility

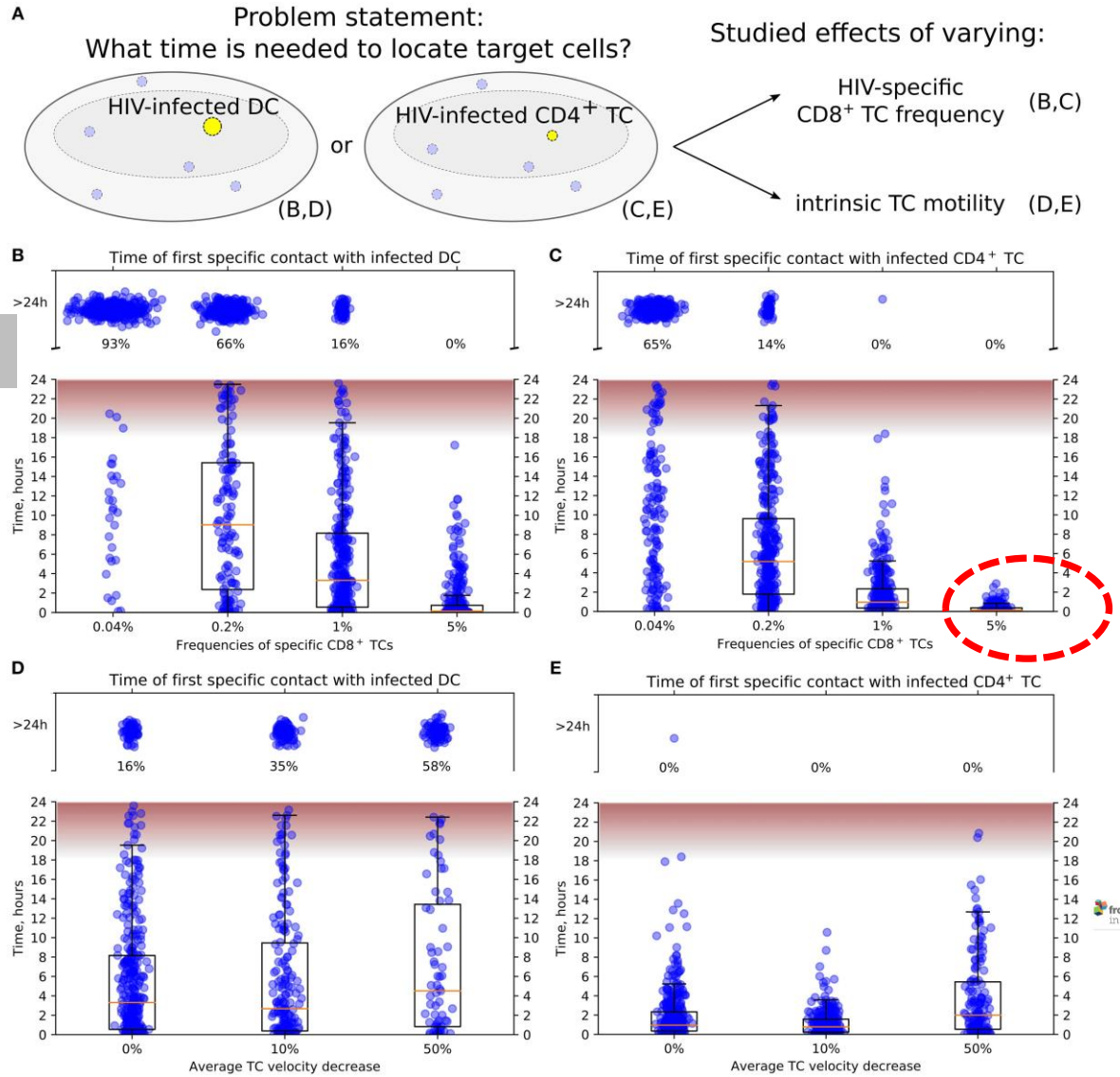

5% of CTLs

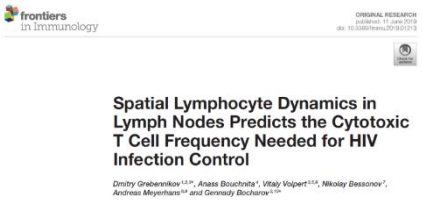

Predictions

The **frequency of HIV-specific CTLs to timely detect** productively infected

- DC within 18 h should be about 5%. The time reduces to 4 h for productively infected CD4+ T cells, which are motile.
- For an HIV-specific T-cell frequency of 1%, the two-fold inhibition of CTL locomotion would reduce the probability of detection of infected ells within 24 h post-cell infection from 0.84 to 0.42.

Platform for hybrid multiscale modelling of HIV infection

Vitaly Volpert and Anass Bouchnita

The immune response to HIV

Nina Bhardwaj, Florian Hladik and Susan Moir

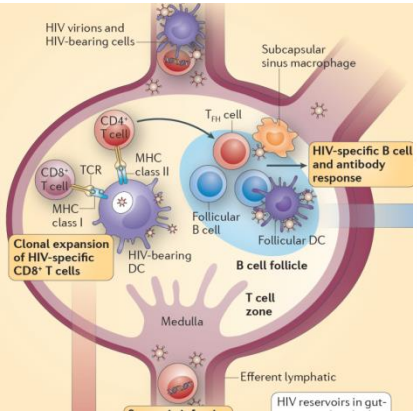

nature REVIEWS IMMUNOLOGY

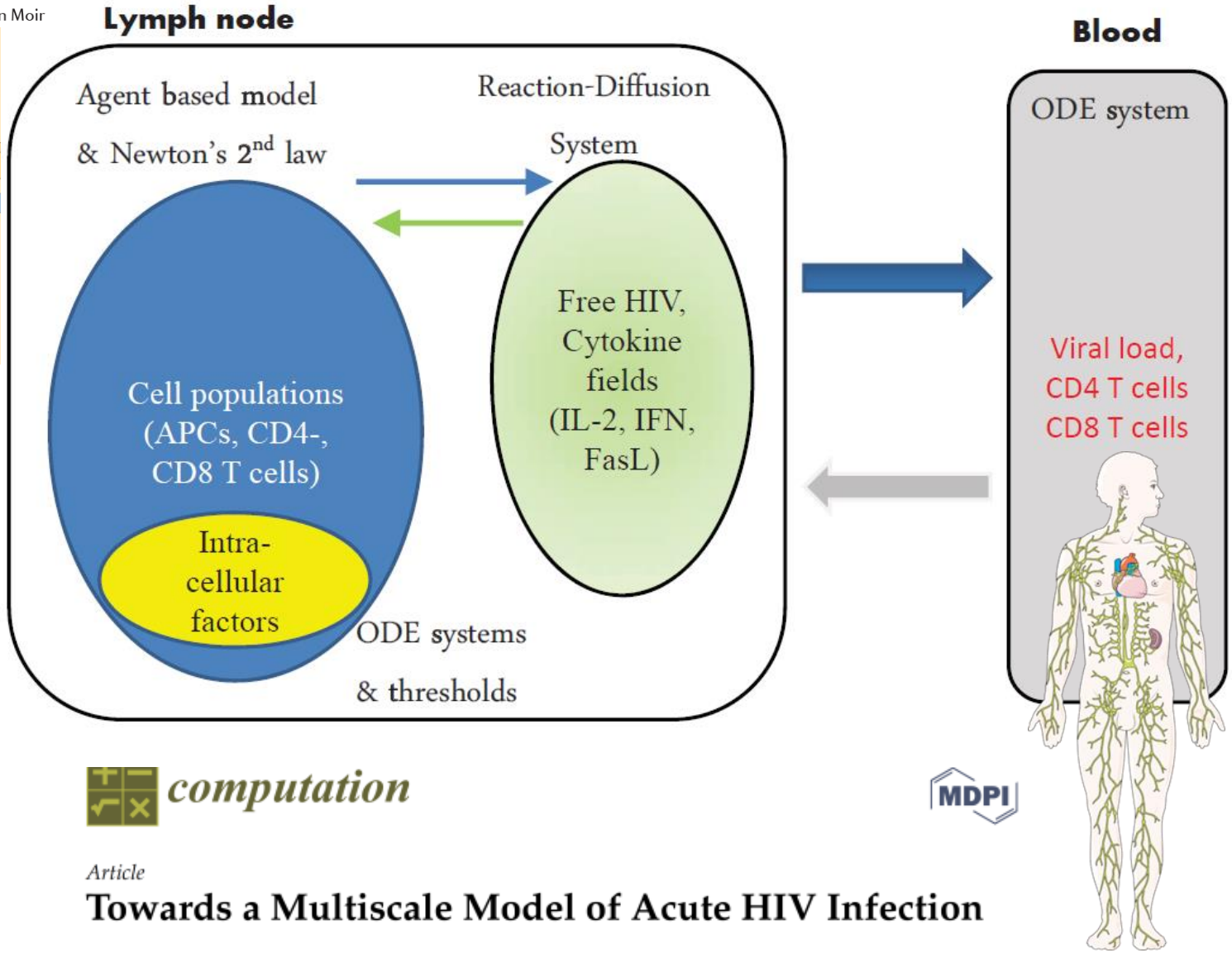

computation

MDPI

Article

Towards a Multiscale Model of Acute HIV Infection

Anass Bouchnita [1,2,3], Gennady Bocharov [4,*], Andreas Meyerhans [4,5] and Vitaly Volpert [1,4,6,7]

Multiphysics model of HIV-1 infection

T cell migration in LN

$$m_i\ddot{\mathbf{x}}_i = \mathbf{F}_i = \sum_{j\neq i} \mathbf{f}_{ij} + \mathbf{f}_i^{mot} - \mu\dot{\mathbf{x}}_i \quad \text{in} \quad \Omega \subset \mathbb{R}^2$$

$$\mathbf{f}_{ij}(h_{ij}) = \frac{\mathbf{x}_i - \mathbf{x}_j}{h_{ij}} \cdot \begin{cases} -a \cdot f_i^{adh}\frac{L-h_{ij}}{L} + b \cdot f_i^{adh}\frac{(L-h_{ij})}{L^3}, & h_{ij} < L, \\ 0, & h_{ij} \geqslant L, \end{cases}$$

Cytokine and HIV-1 fields

$$\frac{\partial c}{\partial t} = D_c\Delta c + s_c - d_c c \quad \text{in} \quad \Omega_D,$$

$$c(\mathbf{x},t) = 0 \ \text{ on } \ \partial\Omega_D, \ c(\mathbf{x},0) = 0 \ \text{ in } \ \Omega_D,$$

Grebennikov et al., 2019

Infection transmission cell-to-cell and free virion-to-cell

$$P(\tau|t^*) = \exp\left(-\int_{t^*}^{t^*+\tau} (k_{free}V_{\Omega_i}(t) + k_{cell}N_{neigh}^{(i)}(t))e^{-(t-t_{inf}^{(i)})/t_d}dt\right)$$

Intracellular HIV-1 replication

$$\frac{dV_{gRNAn}}{dt} = [TR]\cdot V_{int} - (2\cdot k_{sp}\cdot(1-\beta f_{Rev}) + k_{exp}\cdot f_{Rev} + d_{RNA})V_{gRNAn},$$

$$\frac{dV_{dsRNAn}}{dt} = k_{sp}\cdot(1-\beta f_{Rev})V_{gRNAn} - (k_{exp} + d_{RNA})V_{dsRNAn},$$

$$\frac{dV_{dsRNA}}{dt} = k_{exp}V_{dsRNAn} - (d_{RNA} + k_{ISG}\cdot b_{ISG})V_{dsRNA},$$

$$\frac{d[Tat]}{dt} = r_{Tat}V_{dsRNA} - d_{Tat}[Tat], \quad \frac{d[Rev]}{dt} = r_{Rev}V_{dsRNA} - d_{Rev}[Rev],$$

$$\frac{dV_{gRNA}}{dt} = k_{exp}\cdot f_{Rev}\cdot V_{gRNAn} - (2\cdot k_{mat} + d_{RNA} + k_{ISG}\cdot b_{ISG})V_{gRNA},$$

$$\frac{dV_{mat}}{dt} = k_{mat}V_{gRNA} - (k_{\rho_V} + d_{HIV})V_{mat},$$

(3)

Russ. J. Numer. Anal. Math. Modelling 2019; 34(5):253–260

Local burst of infection in T cell zone of LN

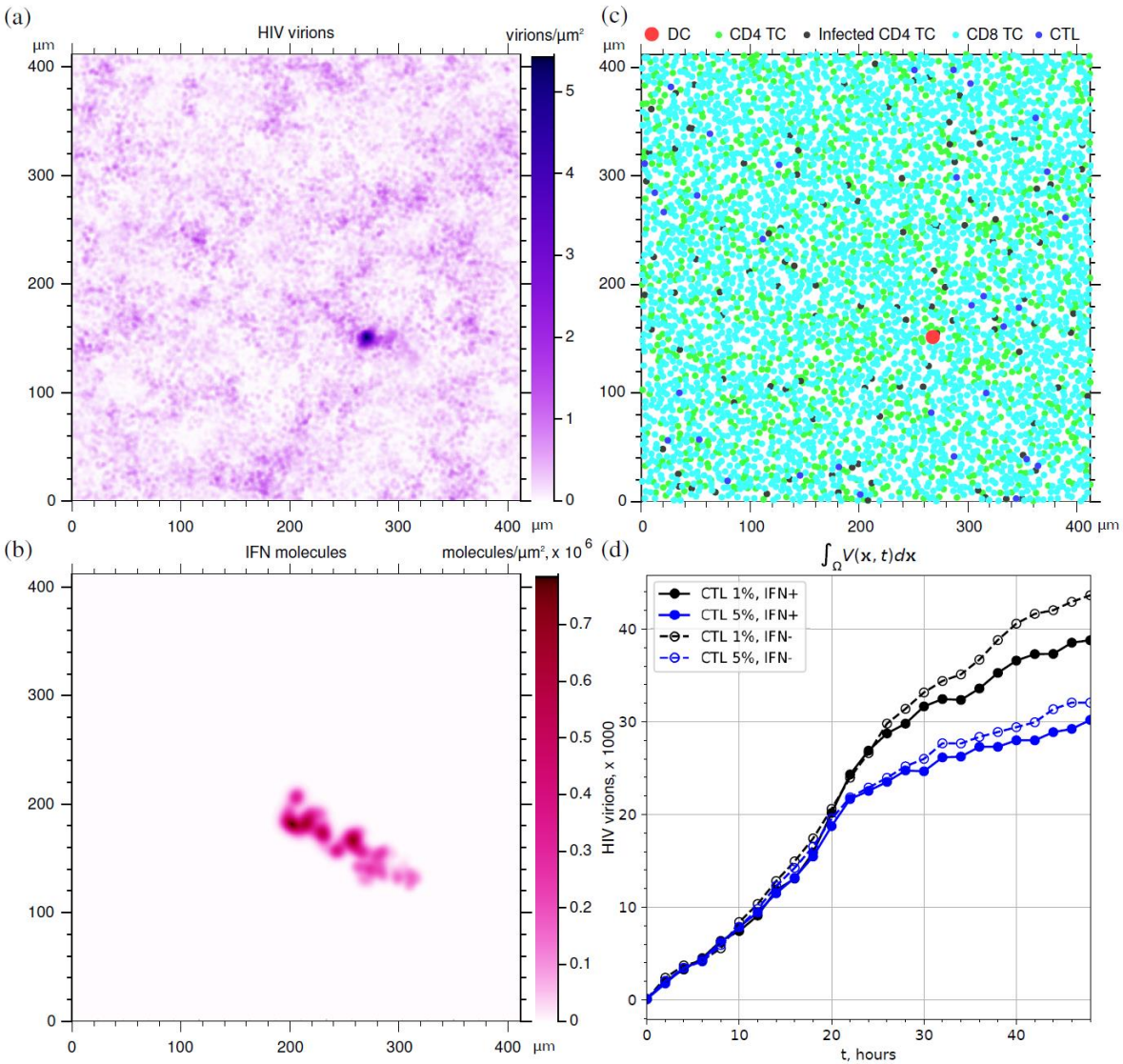

Outline

Исследование робастности защиты системой интерферона при коронавирусной инфекции мышей.

Идентификация новых мишеней для противовирусной терапии ВИЧ-1.

Предсказание терапевтического эффекта блокады рецептора PD-1 в хроническую фазу ВИЧ-1 инфекции.

Исследование влияния подвижности Т-лимфоцитов в лимфатическом узле на эффективность элиминации зараженных клеток при ВИЧ-1 инфекции.

Геометрическое моделирование структурно-функциональной организации лимфатических узлов.

Rostislav Savinkov

Imaging-based analysis of LN structure

PLOS | BIOLOGY

PLoS Biol 14(7): e1002515.

RESEARCH ARTICLE

Topological Small-World Organization of the Fibroblastic Reticular Cell Network Determines Lymph Node Functionality

Mario Novkovic[1☯], Lucas Onder[1☯], Jovana Cupovic[1☯], Jun Abe[2], David Bomze[1], Viviana Cremasco[3], Elke Scandella[1], Jens V. Stein[2], Gennady Bocharov[4], Shannon J. Turley[5], Burkhard Ludewig[1]*

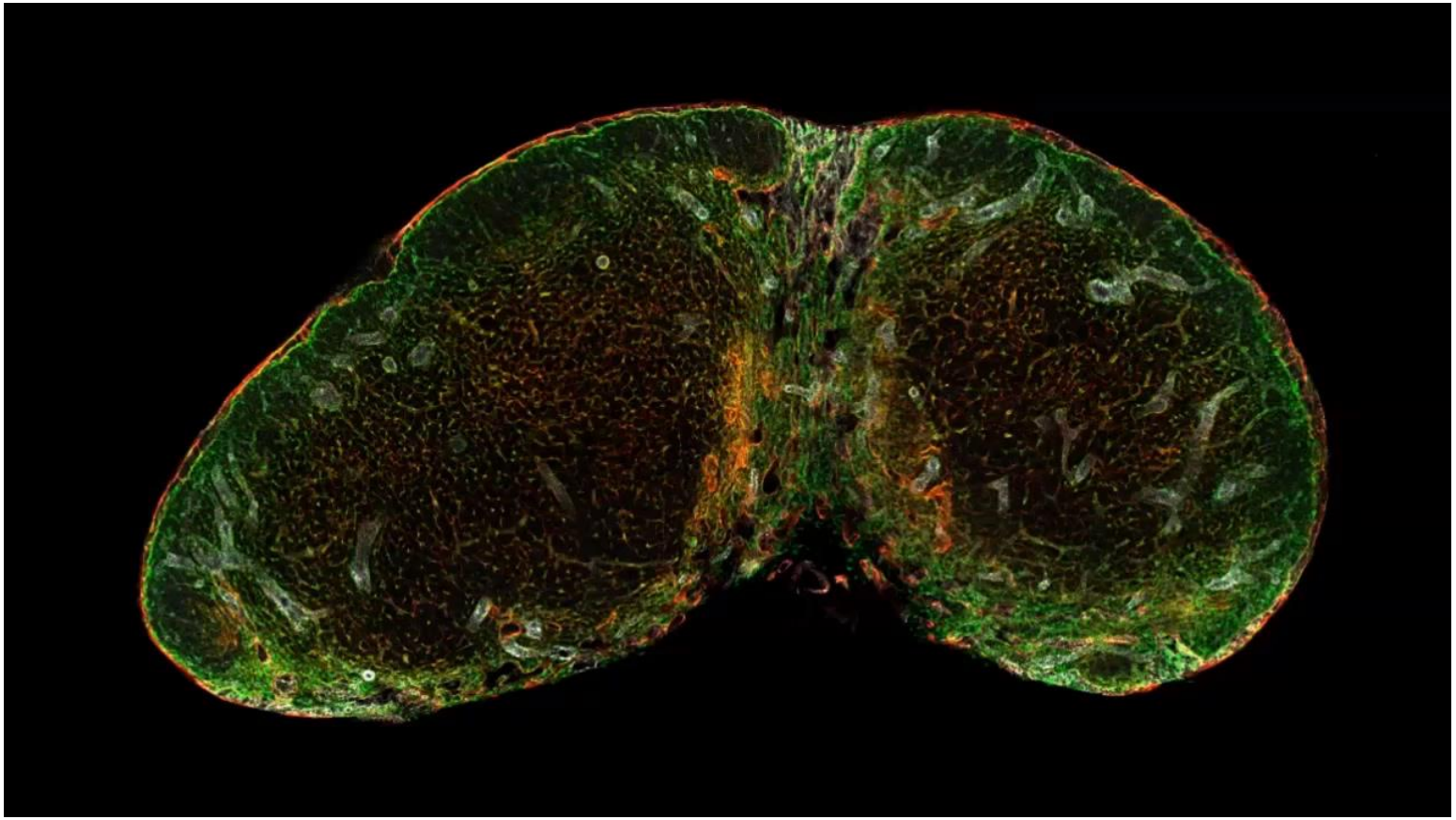

Imaging and visualization of LN structures

Rostislav Savinkov

Experimental data

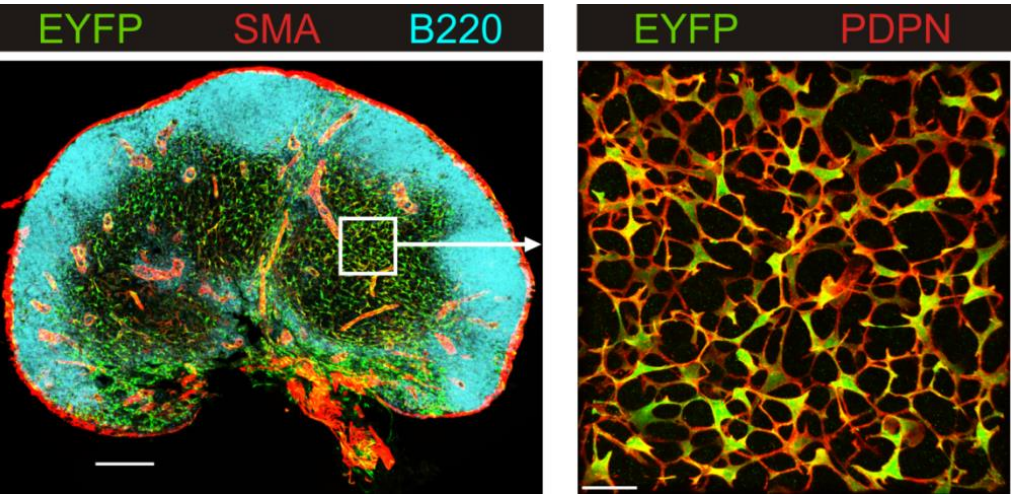

Lymph node (LN) architecture with major structural units: subcapsular sinus (red), efferent lymphatic vessel (red), B cell follicles (cyan) and the FRC network (green). White rectangle indicates representative T cell zone. Scale bar represents 200 µm

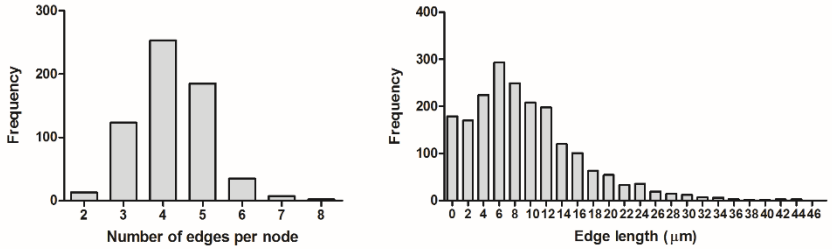

FRC network topology parameters: the edges per node- and the edge length for the T cell zone FRC network. Data obtained from *n* = 7 mice from two independent experiments

Kislitsyn, A.; Savinkov, R.; Novkovic, M.; Onder, L.; Bocharov, G. Computational Approach to 3D Modeling of the Lymph Node Geometry. *Computation* **2015**, *3*, 222-234.

Topology - geometry – 3D solid model

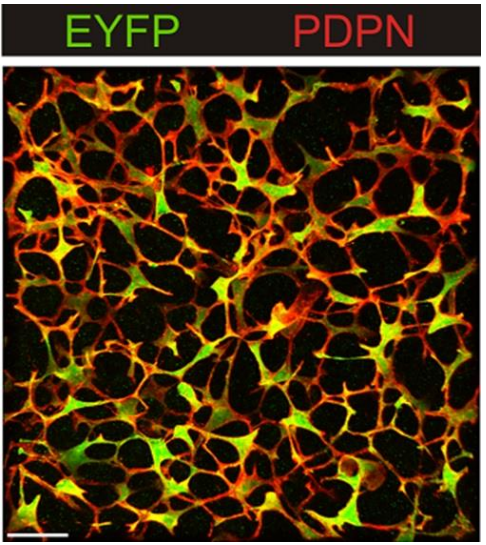

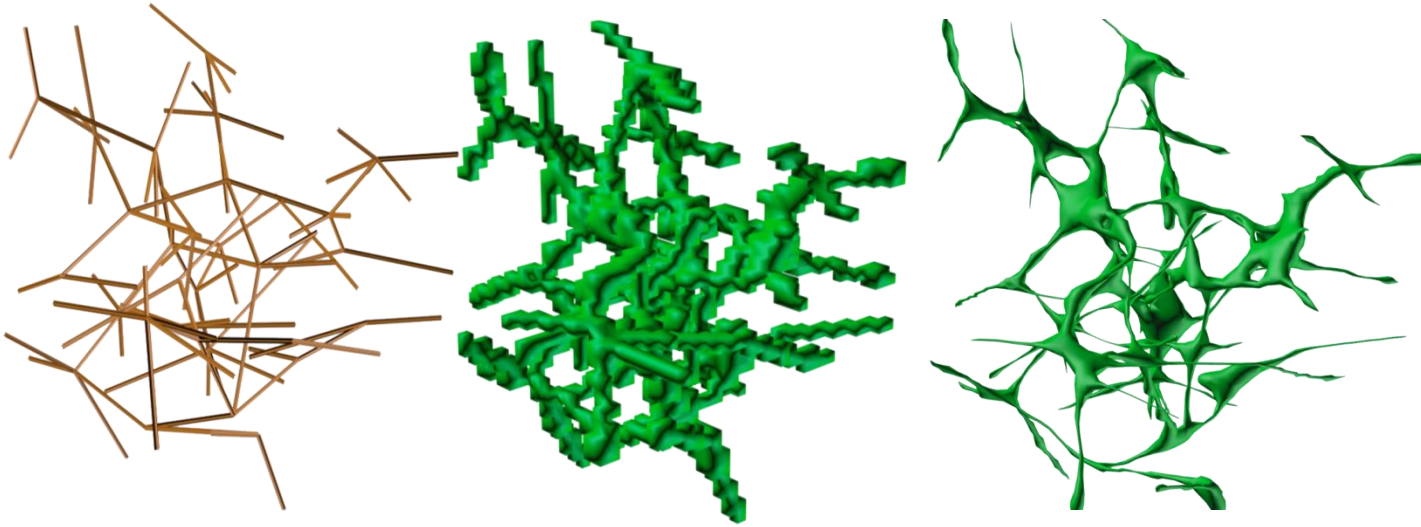

Real Object

Computational model

Voxel-based generation of the FRC network. The network graph model; initial local structure; smoothed solid model of the local structure.

Model of the FRC network graph

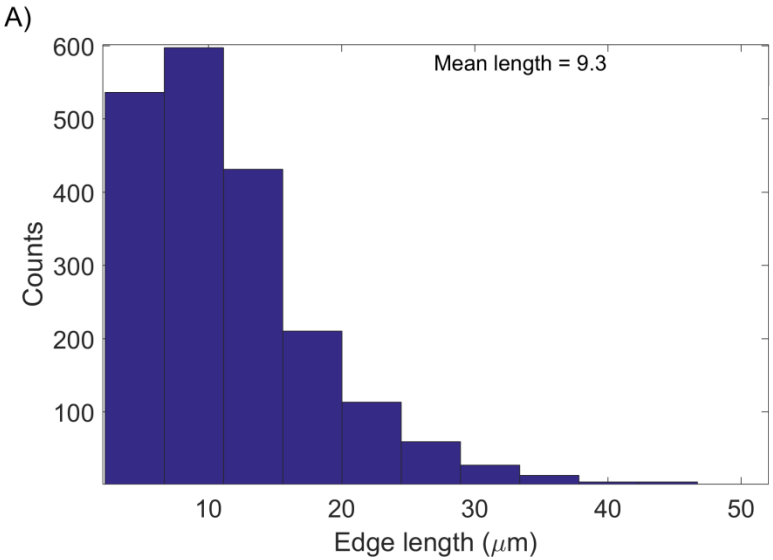

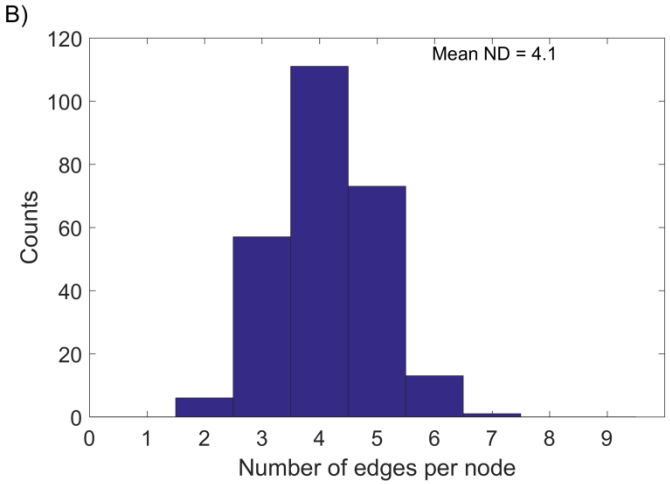

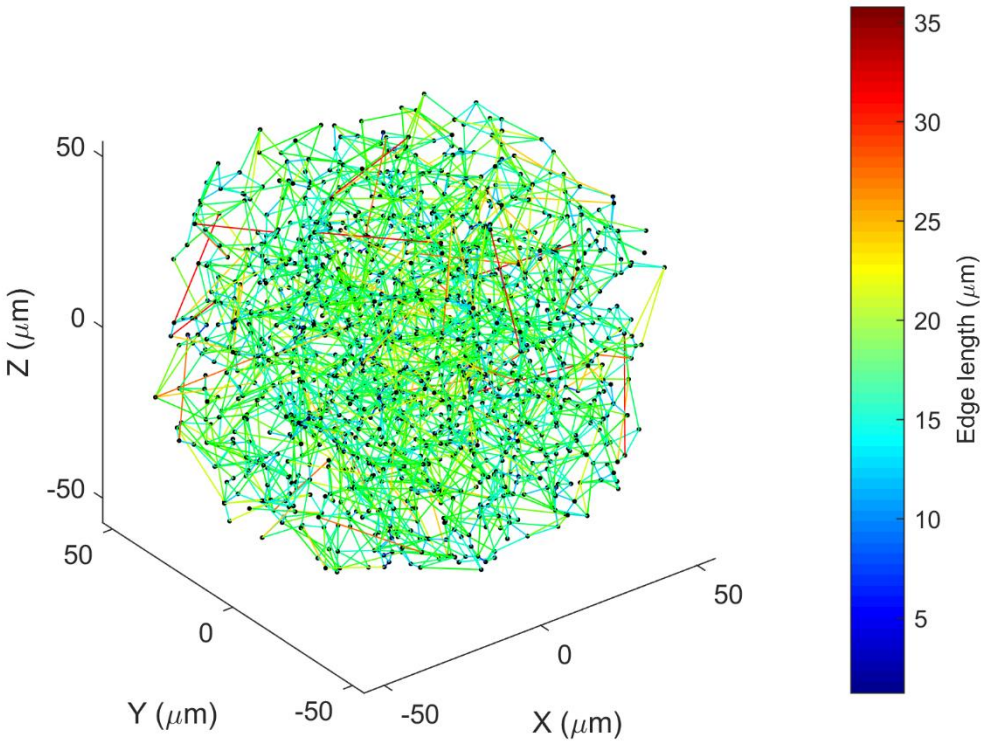

Computational 3D model of the Lymph Node

The FRC and Blood vascular networks inside LN

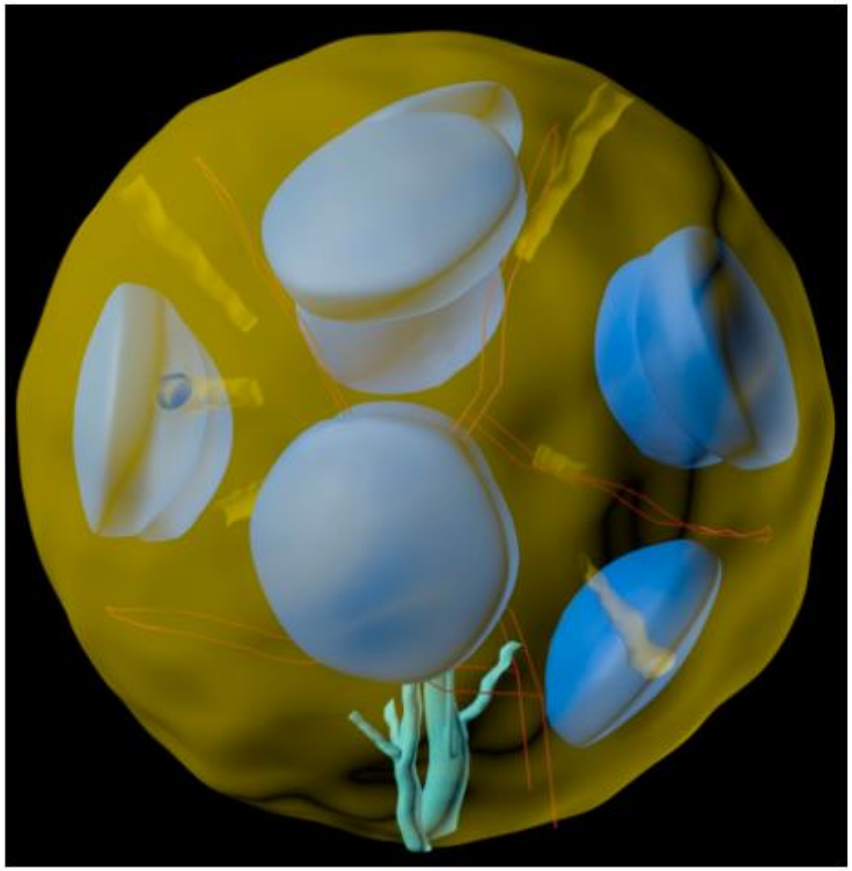

B cell follicles, trabecular sinuses, medulla

Grebennikov, D.; Van Loon, R.; Novkovic, M.; Onder, L.; Savinkov, R. et al. Critical Issues in Modelling LN Physiology. *Computation* **2017**, *5*, 3.

computation
ISSN 2079-3197
www.mdpi.com/journal/computation

Communication

Computational Approach to 3D Modeling of the Lymph Node Geometry

Alexey Kislitsyn [1,†], Rostislav Savinkov [1,†], Mario Novkovic [2,†], Lucas Onder [2] and Gennady Bocharov [3,*]

Immune Flow cytometry data

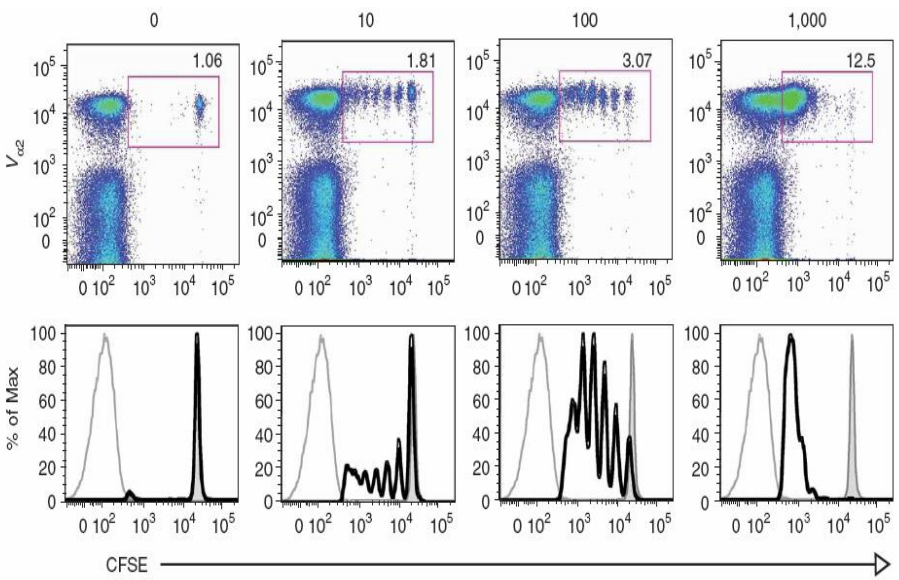

Quah et al., Nat Protoc.2007;2:2049

FlowJo is a product of Tree Star, Inc.
www.flowjo.com
1-541-201-0022
flowjo@treestar.com
TN.Proliferation.20100424

Problem: an interpretation of flow cytometry data

Asymmetric division of lymphocytes

Tatyana Luzyanina

FlowJo is a product of Tree Star, Inc.
www.flowjo.com
1-541-201-0022
flowjo@treestar.com
TN.Proliferation.20100424

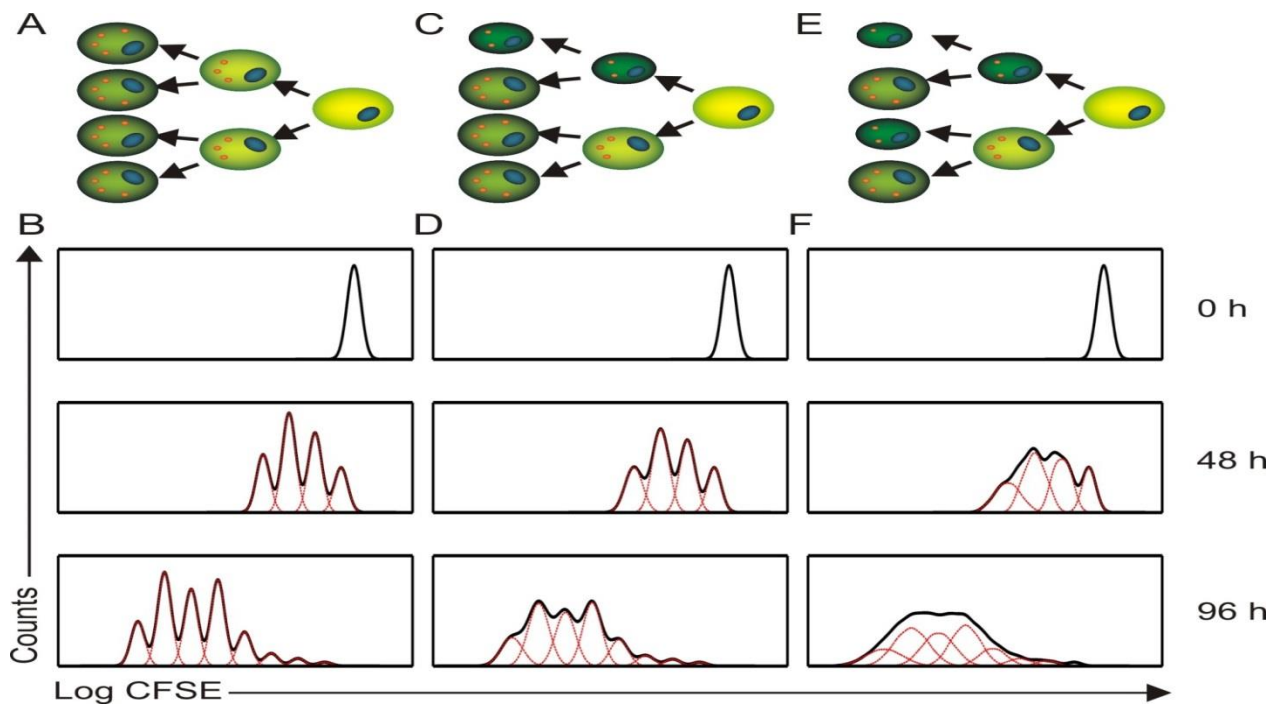

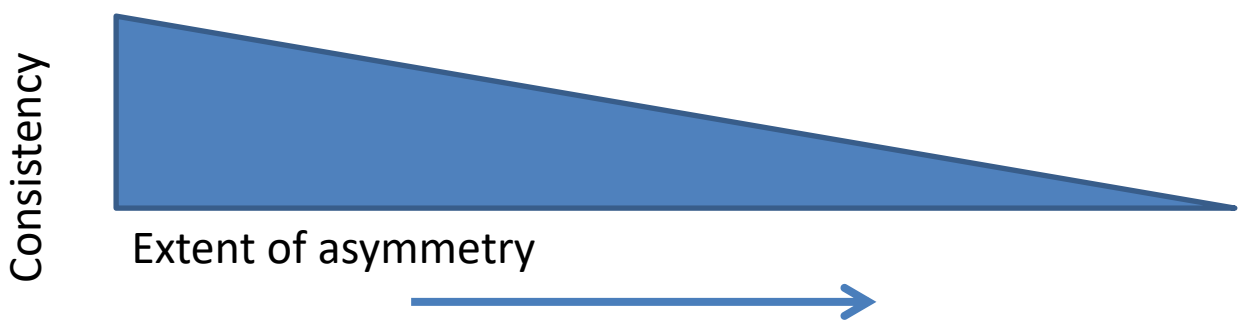

Proliferation of retrogenic CD8+ T cells

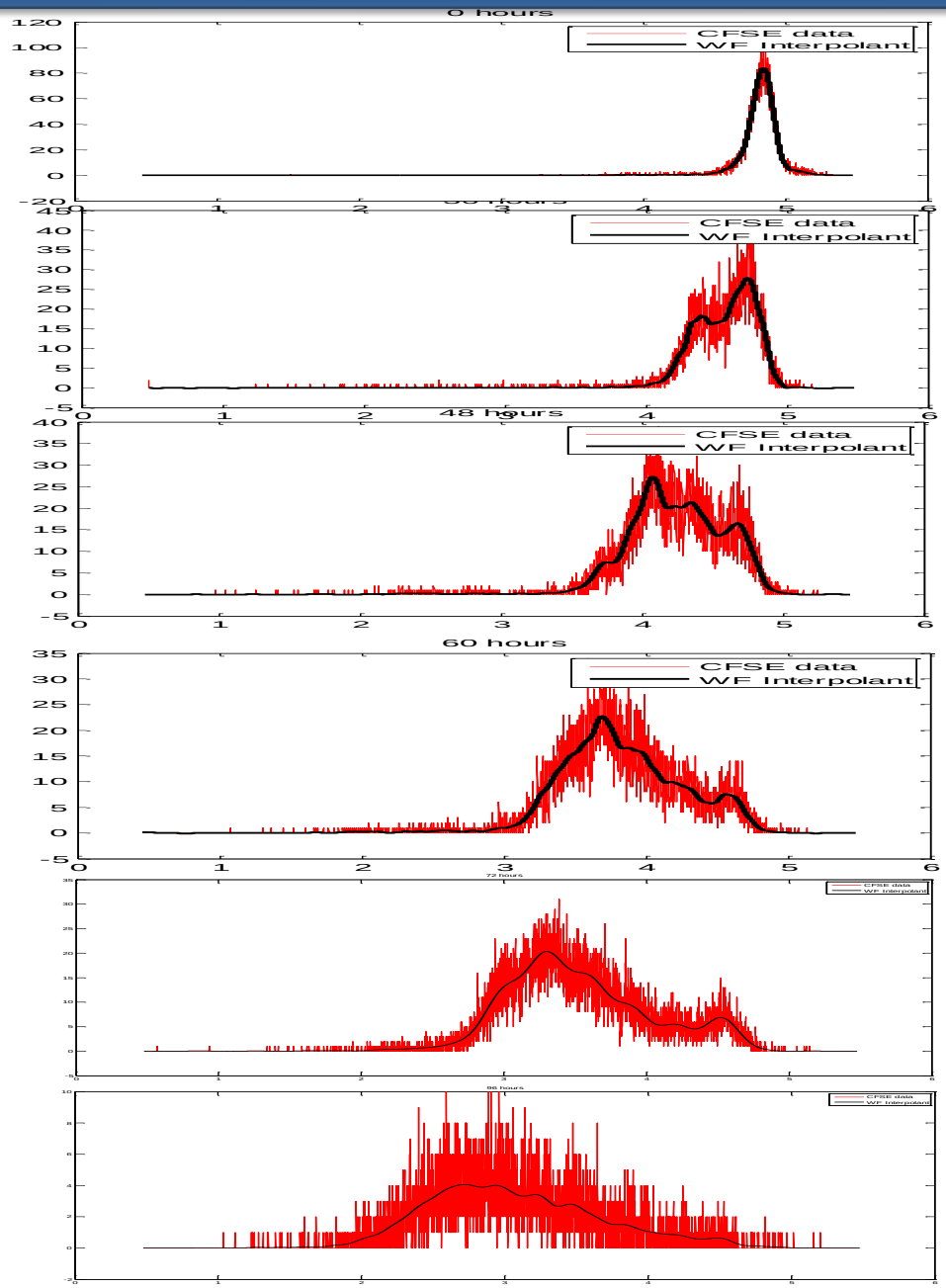

48

60

72

96

Time (hours)

Division number- and label- structured description: *Hasenauer et al. 2011; Banks et al. 2012*

$$\begin{tikzcd}
N(t) \arrow[r] \arrow[d] & N(t, \text{division number}) \arrow[d] \\
N(t,x) \arrow[r] & N(t,x,\text{division number})
\end{tikzcd}$$

$$\frac{\partial N_0(t,x)}{\partial t} - \frac{\partial\big(v(x)N_0(t,x)\big)}{\partial x} = -\big(\alpha_0(t)+\beta_0(t)\big)N_0(t,x),$$

$$\frac{\partial N_i(t,x)}{\partial t} - \frac{\partial\big(v(x)N_i(t,x)\big)}{\partial x} = -\big(\alpha_i(t)+\beta_i(t)\big)N_i(t,x) + 2\gamma\alpha_{i-1}(t)N_{i-1}(t,\gamma x), \quad 1 \le i \le J,$$

$$N_i(0,x) = N_i^0(x),\ v(x_{\min})N_i(t,x_{\min}) = 0,\ 0 \le i \le J,\ \alpha_J(t) = 0,$$

$$t \in [0,T],\ x \in [x_{\min},+\infty)$$

Division- and CFSE-label structured mathematical model

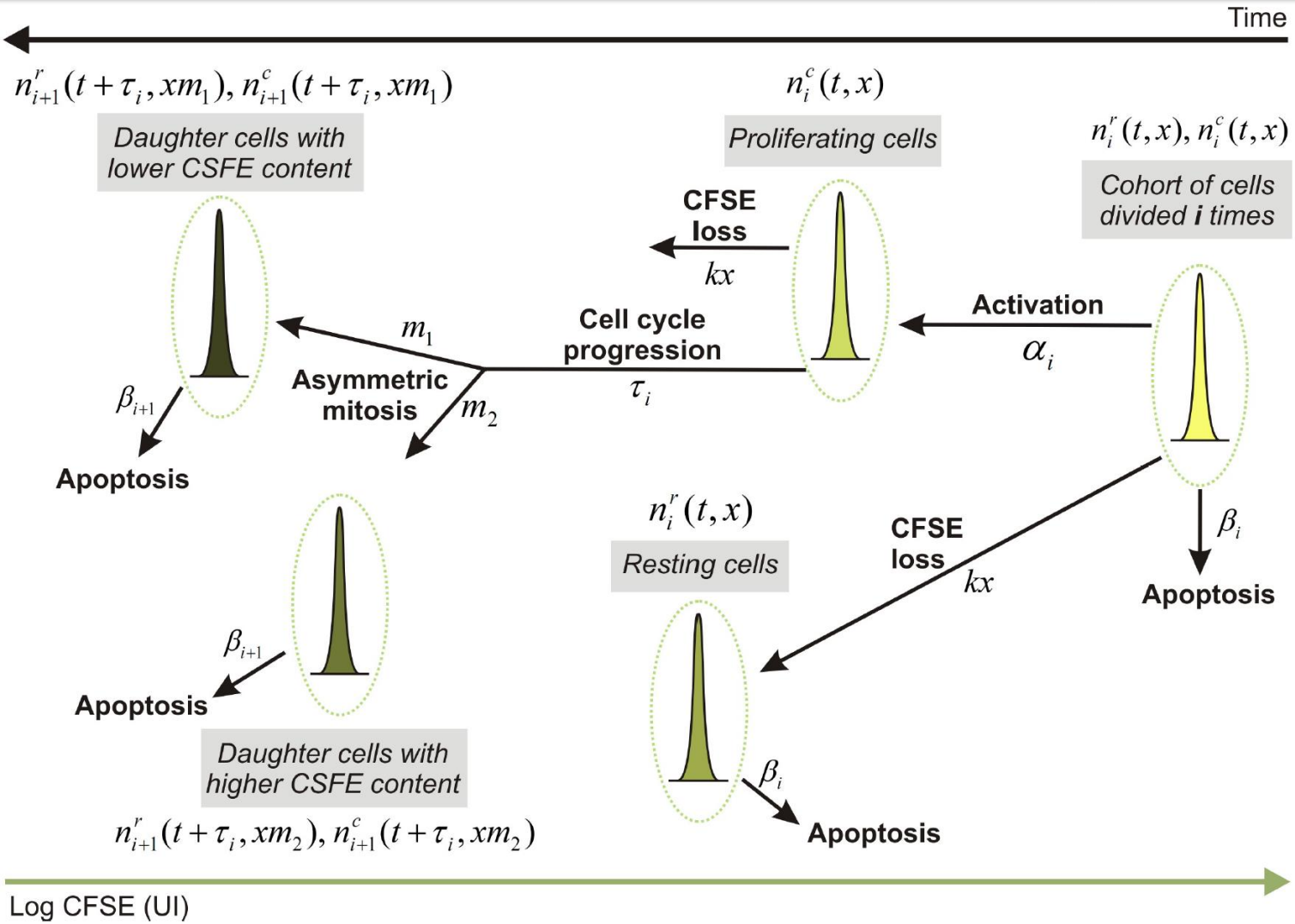

Time-delay hPDE model for asymmetric cell division

$$n_i(t,x) = n_i^r(t,x) + n_i^c(t,x), \quad i = 0,1\ldots,i_p - 1,$$

$$n_{i_r}(t,x) = n_{i_r}^r(t,x)$$

$$\frac{\partial}{\partial t} n_0^r(t,x) - k\frac{\partial}{\partial x}\left(x n_0^r(t,x)\right) = -(\alpha_0 + \beta_0) n_0^r(t,x),$$

$$\frac{\partial}{\partial t} n_i^r(t,x) - k\frac{\partial}{\partial x}\left(x n_i^r(t,x)\right) = -(\alpha_i + \beta_i) n_i^r(t,x) +$$

$$+\alpha_{i-1} e^{k\tau_{i-1}}\left(\frac{1}{m_1} n_{i-1}^r(t-\tau_{i-1}, e^{k\tau_{i-1}}\frac{x}{m_1}) + \frac{1}{1-m_1} n_{i-1}^r(t-\tau_{i-1}, e^{k\tau_{i-1}}\frac{x}{1-m_2})\right), i = 1,2,\ldots,i_r,$$

$$\frac{\partial}{\partial t} n_i^c(t,x) - k\frac{\partial}{\partial x}\left(x n_i^c(t,x)\right) = \alpha_i\left(n_i^r(t,x) - e^{k\tau_i} n_i^r(t-\tau_i, e^{k\tau_i} x)\right), i = 0,1,\ldots,i_r - 1,$$

$$n_0^r(s,x) = 0,\ s \in [-\tau_0, 0);\ n_0^r(0,x) = n^0(x);$$

$$n_i^r(s,x) = 0,\ s \in [-\tau_i, 0],\ i = 1,2,\ldots,i_r;$$

$$n_i^c(s,x) = 0,\ s \in [-\tau_i, 0],\ i = 0,1,\ldots,i_r - 1;$$

$$n_i^r(t, x_{\max}) = n_i^c(t, x_{\max}) = 0,\ t \geq 0;$$

$$v(0) n_i^r(t,0) = v(0) n_i^c(t, x0) = 0,\ t \geq 0;$$

Label- and division- structured time-delay model for an asymmetric cell division

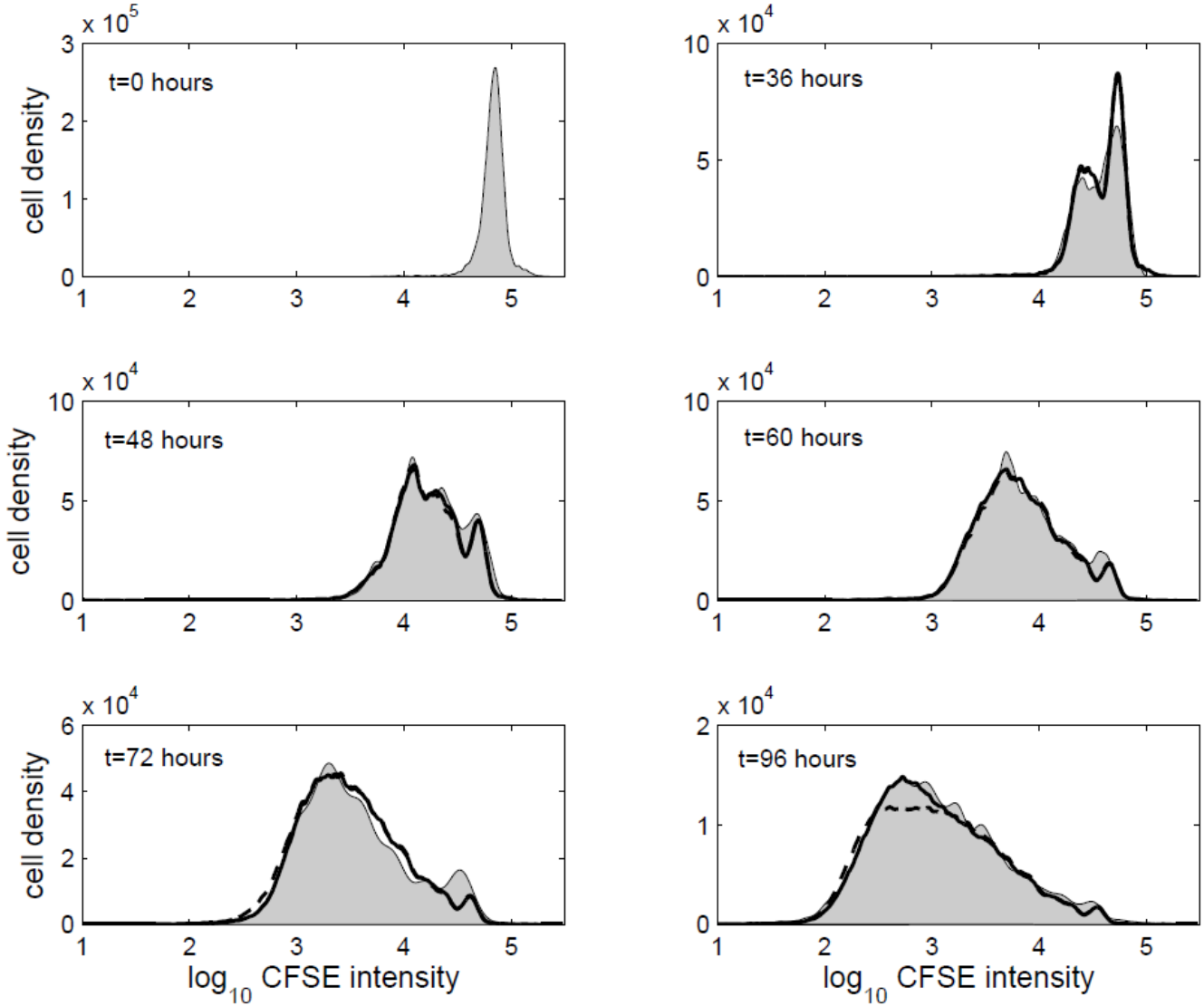

Label- and division- structured symmetric cell division

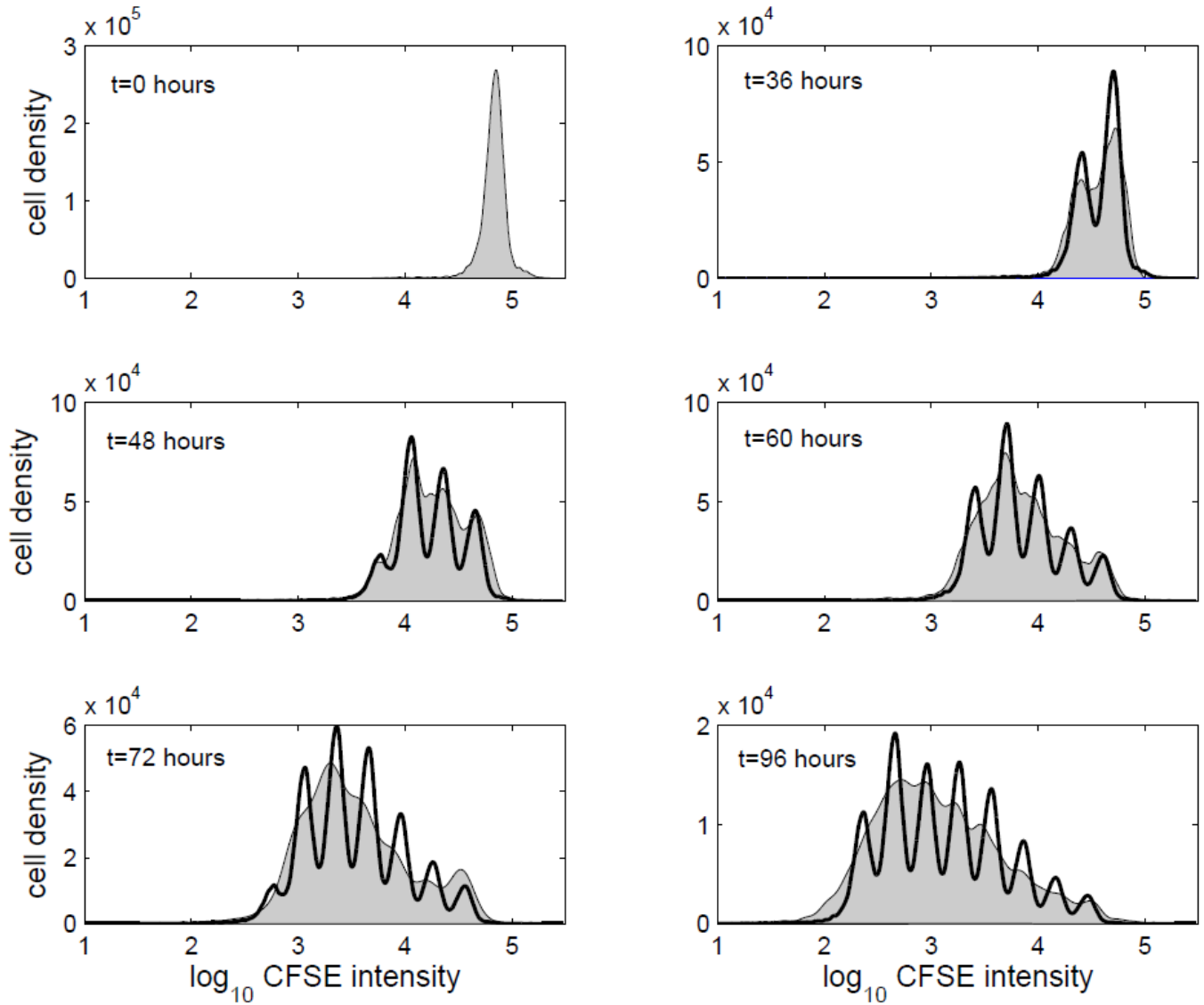

Steady-state solutions: existence of multistability and their robustness

- Dependence on virus–host interaction parameters
- Stability with respect to perturbations

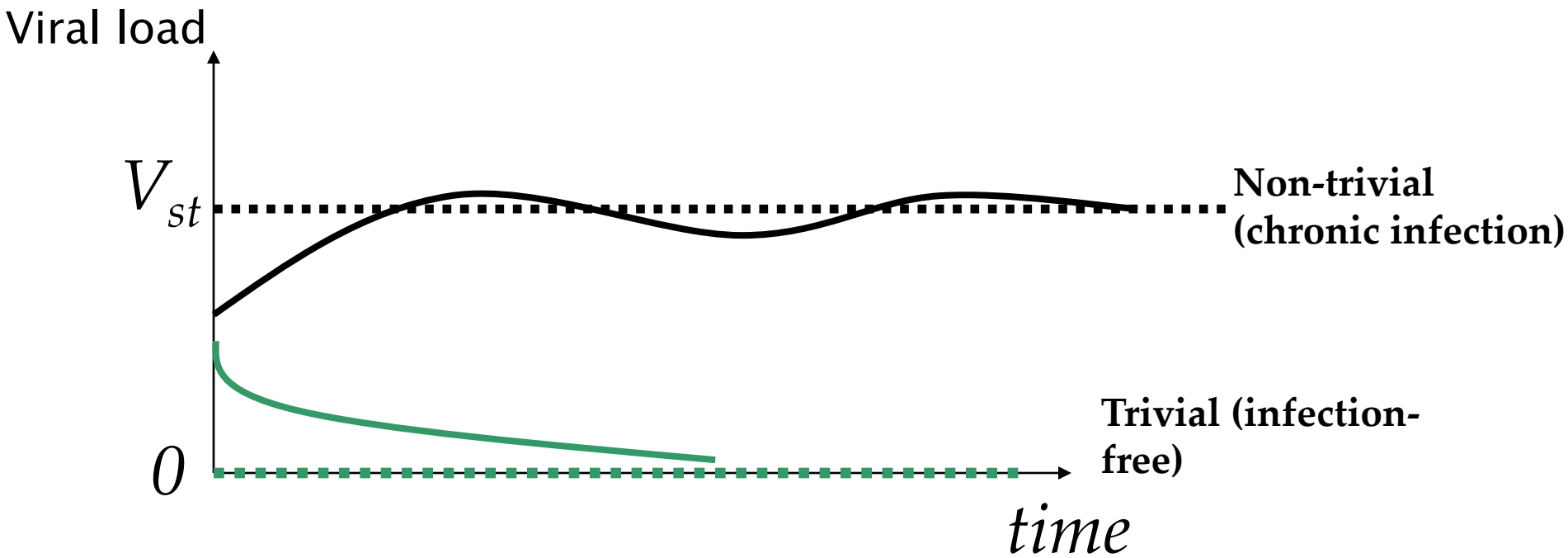

Control of chronic infections: optimal disturbances vs optimal control/stabilization

Arkadii Kim
Yuri M. Nechepurenko
Michael Yu. Khristichenko

Viral load

High viral load steady state

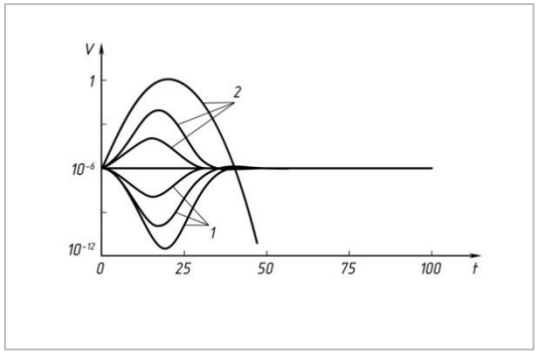

u(t)

Low viral load steady state

Immune status

Virus-free steady state

Viral load

Total amount of drugs

Level of immune memory

Restoration of Immune homeostasis

DE GRUYTER Russ. J. Numer. Anal. Math. Modelling 2017; 32 (5): 275–291

Gennady A. Bocharov*, Yuri M. Nechepurenko, Michael Yu. Khristichenko, and Dmitry S. Grebennikov

Maximum response perturbation-based control of virus infection model with time-delays

Ongoing major research directions

- Intracellular regulation of lymphocyte fate and the immune cell networks homeostasis (**Andreas Meyerhans**)
- Non-local interactions in the immune system (**Vitaly Volpert, Nickolay Bessonov**)
- Anatomically-based and compartmental models considering the phenotypic heterogeneity of the immune cells and stochastic processes (**Nikolai Pertsev**)
- Bifurcation analysis and design of multicomponent personalized therapies (**Yuri Nechepurenko**)
- Optimal control and stabilization of dynamics of virus infections (**Arkadii Kim, Alexey Ivanov**)
- Chronic infections and multifactorial diseases, e.g., SEPSIS (**Willi Jäger**)

Г.И. Марчук:

“…будущее медицины - лечение индивидуального больного на основе слежения за его индивидуальными иммунологическими эндокринологическими и сосудистыми особенностями……”

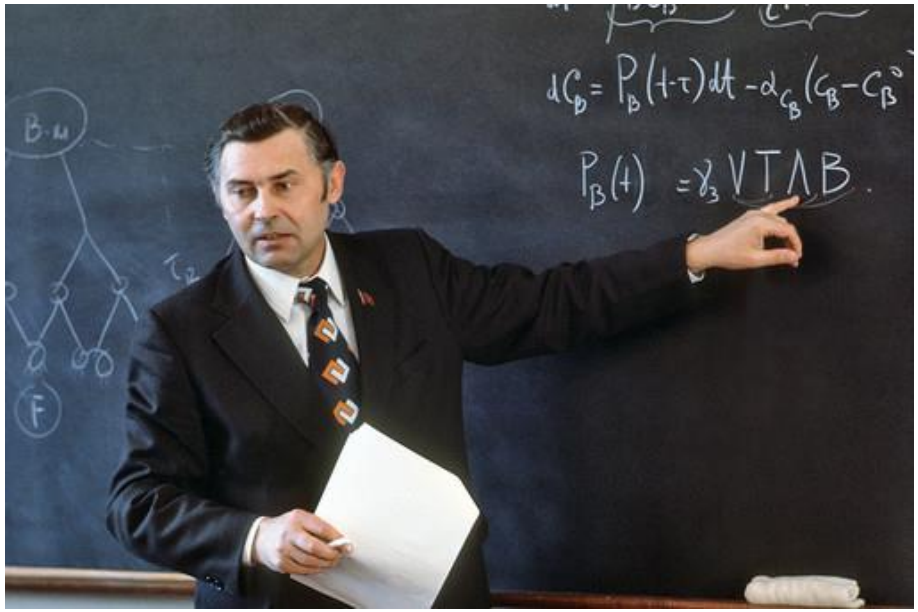

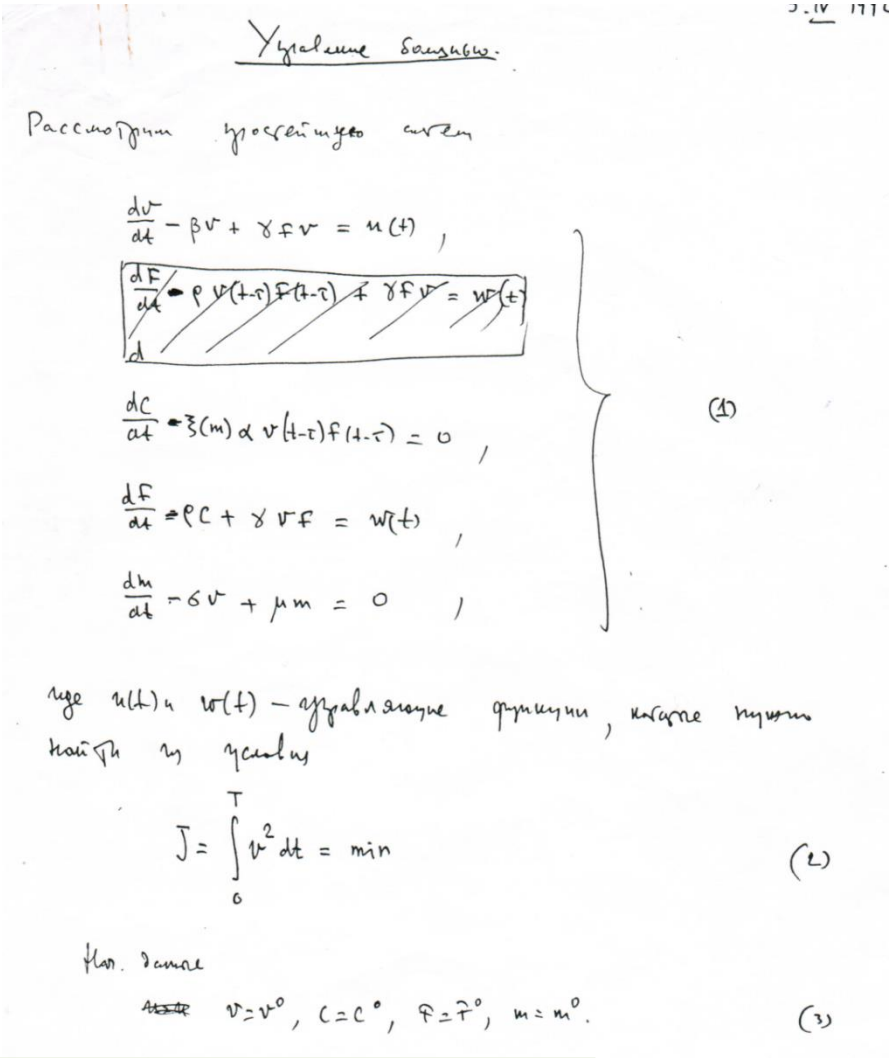

Управление болезнью.

Рассмотрим простейшую систему

$$\frac{dv}{dt} - \beta v + \gamma f v = u(t),$$

$$\cancel{\frac{dF}{dt} - \rho v(t-\tau) F(t-\tau) + \gamma F v = w(t)}$$

$$\frac{dC}{dt} - \xi(m)\alpha v(t-\tau) f(t-\tau) = 0,$$

$$\frac{df}{dt} - \rho C + \gamma v f = w(t),$$

$$\frac{dm}{dt} - \sigma v + \mu m = 0, \qquad (1)$$

где $u(t)$ и $w(t)$ — управляющие функции, которые нужно найти из условия

$$J = \int_0^T v^2 dt = \min \qquad (2)$$

Нач. данные

$$v = v^0, \quad C = C^0, \quad f = f^0, \quad m = m^0. \qquad (3)$$

Спасибо за внимание!

Acknowledgements

Institute of Immunobiology, St. Gallen (Switzerland)
Burkhard Ludewig, Tobias Junt, Philippe Krebs, Lucas Onder, Mario Novkovic

Infection Biology Laboratory, Universitat Pompeu Fabra, Barcelona (Spain)
Andreas Meyerhans, Jordi Argilaguet

Moscow Institute of Physics and Technology, Moscow
Dmitry S. Grebennikov, Olga G. Shcherbatova

Lomonosov Moscow State University Rostislav S. Savinkov, Rufina M. Tretyakova, Valerya V. Zheltkova

Institut Camille Jordan, University Lyon, Lyon (France)
Anass Bouchnita, Vitaly A. Volpert

Institute of Problems of Mechanical Engineering RAS (Saint Petersburg) Nickolai M. Bessonov

Marchuk Institute of Numerical Mathematics RAS
Yuri M. Nechepurenko, Michael Khristichenko, Ekaterina Sklyarova

Sobolev Institute of Mathematics SB RAS Nikolay V. Pertsev, Irina A. Gainova, Konstantin K. Loginov

ГНЦ ВБ Sergey I. Bazhan

Krasovskii Institute of Mathematics and Mechanics (Ekaterinburg)
Arkadii V. Kim

Institute of Immunology and Physiology (Ekaterinburg)
Valery A. Chereshnev

Funding:

Thank you for your attention